ShakeOut Scenario Appendix F: Seismically Induced Landslide Hazard Analysis and Deformation at Lifeline Crossings

By Rick I. Wilson[1], Timothy P. McCrink[1], Jerome A. Treiman[1], and Michael A. Silva[1]

USGS Open File Report 2008-1150, Appendix F
CGS Preliminary Report 25F

2008

U.S. Department of the Interior
U.S. Geological Survey

California Department of Conservation
California Geological Survey

[1] **California Geological Survey**

U.S. Department of the Interior
DIRK KEMPTHORNE, Secretary

U.S. Geological Survey
Mark D. Myers, Director

State of California
ARNOLD SCHWARZENEGGER, Governor

The Resources Agency
MIKE CHRISMAN, Secretary for Resources

Department of Conservation
Bridgett Luther, Director

California Geological Survey
John G. Parrish, Ph.D., State Geologist

U.S. Geological Survey, Reston, Virginia 2008

For product and ordering information:
World Wide Web: http://www.usgs.gov/pubprod
Telephone: 1-888-ASK-USGS

For more information on the USGS—the Federal source for science about the Earth, its natural and living resources, natural hazards, and the environment: World Wide Web: http://www.usgs.gov
Telephone: 1-888-ASK-USGS

Suggested citation:
Wilson, Rick I., McCrink, Timothy P., Treiman, Jerome, Silva, Michael A., 2008, ShakeOut Scenario Appendix F; Seismically induced landslide hazard analysis and deformation at lifeline crossings, Appendix F *of* Jones, L.M., The ShakeOut Scenario: U.S. Geological Survey Open-File Report 2008-1150, and California Geological Survey Preliminary Report 25F, 60 p.
[http://pubs.usgs.gov/of/2008/1150/appendixes/of2008-1150_appendix_f.pdf].

ShakeOut Scenario
Appendix F.
Seismically-Induced Landslide Hazard Analysis and Deformation at Lifeline Crossings for the M7.8 Southern San Andreas Earthquake Scenario

Rick I. Wilson, Timothy P. McCrink, Jerome A. Treiman, and Michael A. Silva
California Geological Survey

The Multi-Hazard Demonstration Project (MHDP) is an "earthquake planning scenario" for a 7.8 magnitude event on the south-central segment of the San Andreas Fault, rupturing from Bombay Beach at the north end of the Salton Sea, to Lake Hughes in the Transverse Range. The California Geological Survey (CGS) analyzed earthquake ground deformation hazards in select focus areas where numerous utility and transportation lifelines either cross or are near the area of the scenario fault rupture. The focus areas examined by CGS are Interstate 5 near Pyramid Lake (Tejon Pass), Palmdale/Highway 14 (Soledad Pass), Cajon Pass, San Gorgonio Pass and the Coachella Valley near Indio (Figure 1). Because landslide susceptibility and lifeline impacts were determined to be greater in the Cajon Pass and San Gorgonio Pass, these focus areas were analyzed in more detail than the other areas. Conversely, because landslides were not considered a significant hazard to lifelines in the flat-lying Coachella Valley, landslide hazards were not analyzed in that focus area.

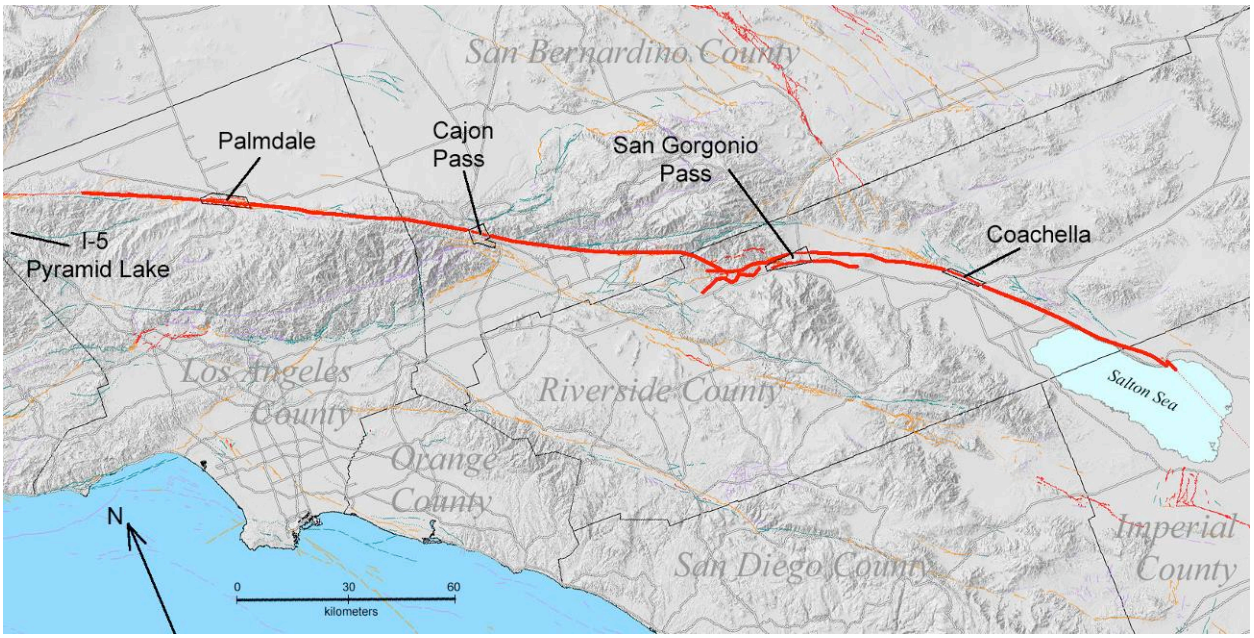

Figure 1. Location of MHDP focus areas evaluated for earthquake triggered landslide hazards in southern California. Dark red line represents segment of the San Andreas Fault that ruptures during the scenario earthquake.

The purpose of this report is to address the potential impacts of landslides and rock falls on lifelines in the focus areas to help project scientists, utility managers, and emergency planners develop their action plan for the MHDP earthquake scenario. The results of this evaluation, therefore, are presented only as estimates of potential slope failure and subsequent damage to lifelines (the "Limitations" section at the end of the report summarizes some of the unknown variables that should be considered when using the results of this report).

Landslide analysis methods varied between the focus areas depending on the significance of the hazard and the data available. This report discusses the possible "worst-case" impacts to railways, overhead transmission lines, petroleum product pipelines, and fiber-optic communication lines in the focus areas. Also discussed are the types of slope failure impacts, ranging from utilities potentially being covered by debris to utilities potentially being disrupted and having complete failure/disruption. As they relate to the individual lifelines, the representative volume of debris deposited and/or amount of displacement are also estimated.

This report considers the results of the slope stability analysis and assesses the potential for one or more of the following lifeline impacts:

1) **Buried by debris** – Occurs where lifelines cross the base of and are not undercut or moved by the landslide. This impact can make lifelines at the surface, like railways, inoperable until the debris is removed, and may have minor impacts on buried utilities.
2) **Lateral displacement** – Occurs where lifelines cross a landslide but the displacement within the landslide or surficial material is not likely significant enough (less than one meter) to cause complete failure. However, even small displacements can cause significant damage to buried utilities (such as pipelines) or railways, but may not cause long-term disruption to highways.
3) **Complete failure** – Occurs were the lifelines cross an existing landslide that loses its internal structure and fails catastrophically. Complete failure is most likely to occur on existing landslides where estimated Newmark displacements are greater than one meter, where there is enough uncertainty about the landslide hazard to error on the side of being conservative, or where lifeline structures, at the surface or buried at a shallow depth, cross an area where significant shallow sliding is expected.

Cajon Pass Focus Area

The Cajon Pass focus area is approximately 20 square kilometers in area and is located along the Interstate 15 corridor about 39 kilometers north of the City of San Bernardino (Figure 2). In this area, the Cajon Canyon forms the boundary between the San Gabriel Mountains to the west and the San Bernardino Mountains to the east. Relief in this area is over 1000 meters with relatively steep mountain fronts dissected by drainages that exhibit seasonal surface-water flow.

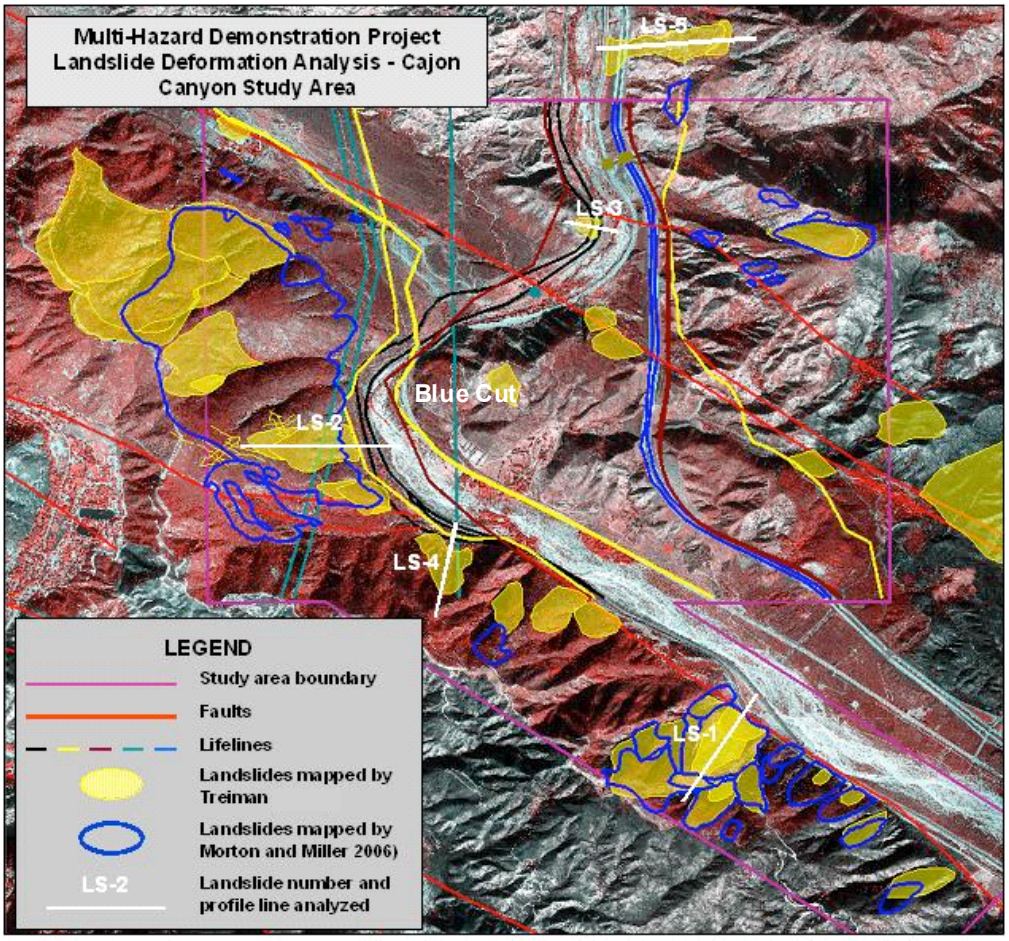

Figure 2. Mapped landslides in the Cajon Pass Focus Area. Landslides outlined in blue are from Morton and Miller (2006). Landslides shaded yellow were mapped for this study by Treiman. The landslides selected for displacement analyses are labeled. Some of the known utilities are shown by lines of different colors. Base map image is a false color infrared orthophoto flown by EarthData in 2003 after the severe fires in this area.

The San Andreas fault crosses the focus area diagonally from the northwest. South of the San Andreas fault, the geology is predominated by the Pelona Schist, a geologic formation well known for being susceptible to landslides. Cretaceous and Tertiary age igneous and sedimentary

rocks make up the majority of the bedrock units north of the San Andreas Fault. Numerous Quaternary terrace and alluvial deposits exist in the canyon areas.

The impacts to lifelines from a similar scenario earthquake for the Cajon Pass area were previously evaluated and summarized in reports published by the Federal Emergency Management Agency (FEMA, 1992a; 1992b).

The two sets of landslide inventories that cover the Cajon Pass focus area that were utilized during this study are shown in Figure 2. Morton and Miller (2006) digital geology of the area contains older and younger landslide deposits (outlined in blue in Figure 2) that had been originally mapped at a 1:24,000 map scale. For this study, Treiman created a landslide inventory (in the yellow shaded areas in Figure 2) based on stereo aerial photograph interpretation. As seen in Figure 2, the two landslide inventories are similar in most areas but vary in interpretation of some of the bigger landslides mapped by Morton and Miller (2006) in the western part of the focus area.

In addition to landslides, Figure 2 shows the location of some of the significant utility and transportation lifelines that pass through the focus area. Lifeline locations for this analysis were initially extracted from a database provided by the Federal Office of Homeland Security [Ken Hudnut (USGS), personal communication]. Black lines represent the two railways that border the western part of the canyon. The yellow lines represent several of the gas and petroleum product pipelines. The brown lines are two of the fiber optic lines that cross the area from north to south. The blue lines show the location of Interstate 15.

The analysis and discussion for Cajon Pass is divided into two parts based on the mode/depth of landslides expected: 1) areas where moderate- to deep-seated landslides were identified, and 2) areas where shallow landslides are expected based on the results from a hazard potential map similar to those created by CGS' Seismic Hazard Zonation Program.

Moderate- To Deep-Seated Landslides

The stability analyses performed for moderate- to deep-seated landslides in this study involved: 1) evaluating and selecting landslides and slopes within the focus area that are most likely to impact roadway, railway, and utility lifelines; 2) creating topographic profiles across selected slopes; 3) inferring subsurface geologic and hydrologic conditions from stereo aerial photograph geomorphic analyses and field reconnaissance, and preparing geologic cross-sections along topographic profiles; 4) performing static slope stability analyses to refine subsurface geologic interpretations and material strength characteristics; 5) performing pseudo-static slope stability analyses to determine yield acceleration for each slope; and 6) using the Bray and Travasarou (2007) procedure to estimate ranges of seismically induced slope (Newmark) displacements.

Several approaches to estimating earthquake-triggered displacements in deep-seated landslides are available. The model chosen for this analysis is a simplified procedure based on fully-coupled sliding block analyses of over 600 recorded earthquake ground motions (Bray and Travasarou, 2007). This model requires six input parameters: 1) site PGA; 2) earthquake magnitude; 3) yield acceleration; 4) average thickness of the sliding mass; 5) average shear wave velocity of the slide mass; and 6) the spectral acceleration at the degraded fundamental period of the slide mass. Parameters 1, 2 and 6 were provided as part of the scenario ground motion estimation. Parameters 3 and 4 were estimated during the slope stability analyses. Average shear wave velocities, parameter 5, were estimated from Fumal and Tinsley (1985) and Wills and Clahan (2006).

Detailed subsurface geologic information and measured material strength properties were sparse or lacking for the slopes and landslides evaluated in this study. In most cases surficial geomorphic analyses were used to identify geologic structures that influenced the type and location of landslide slip surfaces. CGS' existing database of material strength parameters provided a starting point for assessing rock strengths. Possible ground-water seepage noted during field reconnaissance helped define ground water conditions for stability analyses. Slope stability analyses were used to refine the initial assumptions and develop reasonable subsurface geologic configurations and material properties for the displacement analyses.

Five landslides (the labeled landslides in Figure 2) were selected based on their proximity to specific lifelines. A description of the geotechnical properties of the geologic materials that make up the landslides evaluated is presented in Table 1. Topographic profiles of the landslides were obtained from the 2-meter interferometric I-STAR digital elevation model (DEM) flown by EarthData in 2003. A detailed analysis was made to determine their potential for seismically induced failure and what impact they would have on the lifelines nearby.

Table 1. Geologic information and general rock strength characteristics for landslides in the Cajon Pass focus area. Geologic information from Morton and Miller (2006):

LS Number	Geologic Formation	Formation Description	General Rock Strength Characteristics
LS-1A, 1B, and 1C	**Qyls** = Young landslide deposits (Holocene and late Pleistocene) on **Kps** = Pelona Schist, muscovite schist unit	Slope-failure deposits that consist of displaced bedrock blocks and/or chaotically mixed rubble of Pelona Schist. Slightly dissected or modified surfaces.	Although in hand sample the Pelona Schist appears durable, most of this unit is highly fractured and prone to landslides. Many of the landslides that occur in the Pelona Schist are foliation-plane failures that commonly lack classic landslide topography.
LS-2	**Qyls** = Young landslide deposits (Holocene and late Pleistocene) on **Kps** = Pelona Schist, muscovite schist unit	Slope-failure deposits that consist of displaced bedrock blocks and/or chaotically mixed rubble of Pelona Schist. Slightly dissected or modified surfaces.	Although in hand sample the Pelona Schist appears durable, most of this unit is highly fractured and prone to landslides. Many of the landslides that occur in the Pelona Schist are foliation-plane failures that commonly lack classic landslide topography. Although residual shear strength phi values from the the Pelona Schist are usually in the mid 20^{o} range, material from this landslide is older and appears to be more stable than other landslides.
LS-3	**Kgdc** = Biotite granodiorite, Cajon area (Cretaceous)	Medium- to coarse-grained, granodiorite, ranging to monzogranite. Most is massive, tan weathering biotite granodiorite, locally gneissoid.	Slightly gneissic granodiorite in area is highly fractured and weathered, likely due its close proximity to the San Andreas fault zone. As observed in shear strength data collected from landslides in granitic rock from other parts of southern California, pre-existing landslide material typically has a shear strength phi angle in the mid 20^{o} range.
LS-4	**Kps** = Pelona Schist, muscovite schist unit	Spotted muscovite-albite-quartz schist and siliceous schist relatively homogeneous in appearance, well layered, and fissile.	Although in hand sample the Pelona Schist appears durable, most of this unit is highly fractured and prone to landslides. Many of the landslides that occur in the Pelona Schist are foliation-plane failures that commonly lack classic landslide topography.
LS-5	**Tcv5** = Cajon Valley Formation, Unit 5 (Miocene?)	Interbedded (fresh-water?) conglomerate and conglomeratic sandstone, pebbly fine- and coarse-grained sandstone, and siltstone.	Material from this landslide appears more incompetent than that of the surrounding (intact) rock. A shear strength phi-angle value in the mid 20^{o} is representative the fine-grained material from Tertiary interbedded sedimentary formations in Southern California.

Landslide LS-1 (A, B and C)

Location: The LS-1 landslide complex is located in the most southern part of the focus area on the west side of Cajon Wash (Figure 3).

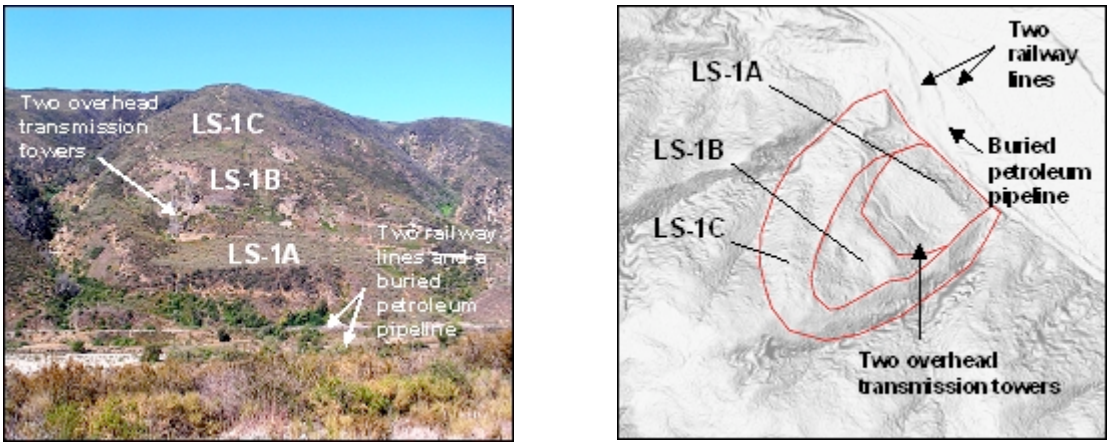

(a) (b)

Figure 3. Parts (A, B, and C) of Cajon Pass focus area Landslide LS-1 observed (a) from the ground and (b) on a shaded relief terrain image. Stream erosion and perhaps railroad construction has removed landslide toes. Additional landslides extend all the way to the top of the ridge but only these three were evaluated for this study.

Notable Physical Features:

- three landslides in one large landslide mass representing three periods of sliding;
- adverse foliation attitudes within Pelona Schist around the landslide appear to exist, dipping to the east, the direction of sliding, at about 45^{o};
- LS-1A is youngest and forms the base of the complex:
  - is in line downslope of LS-1A and LS-1B,
  - has well-developed arcuate and side scarps,
  - has a well formed bench,
  - has oversteepened base caused by natural erosion or grading at toe,
  - contains apparent year-round springs at base and along sides of LS-1C,
  - exact age of LS-1C not known but likely formed between 1966, the year that the topography for USGS 7.5-minute Devore Quadrangle was made, and 2003, when I-STAR interferometric DEM was collected;
- LS-1B is central portion of complex:
  - has arcuate shape and well-formed headscarp,
  - bench has been somewhat modified by erosion,
  - is centered in middle of LS-1A;
- LS-1C is oldest, upper part of landslide complex analyzed:
  - has eroded headscarp and incised lateral sections,
  - has subtle bench (heavily eroded),
  - forms majority of wedge-shaped ridge.

Assumptions for Landslide Displacement Analysis: All three landslides within the complex were analyzed separately for Newmark displacements. Based on the instability within the landslide complex, several assumptions regarding subsurface conditions were formulated:

1) Based on the structural information from the Morton and Miller (2006) geologic map, it appears that foliation within the Pelona Schist in this area dip to the east/northeast, parallel to the steep surface topography, and may form adverse bedding conditions for landsliding. Therefore, eastward-dipping layers that had weaker strengths were added to the landslide cross-section to represent existing landslide slip surfaces within the Pelona Schist.
2) Observed active springs at the base and along the sides of the landslide complex indicate that unconfined ground water table may be a significant factor in sliding. The location of the springs was used to help define the ground-water table.
3) Material strength properties were not available in the Cajon Pass area. Shear strength values for Pelona Schist collected by the CGS Seismic Zonation Program from Los Angeles County were utilized as a guide for strength values used in the slope stability analyses.
4) Shear wave velocities were assigned to the landslides such that they increased with landslide thickness.

LS-1A Analysis: The modeled slope static analysis for LS-1A is shown in the Figure A1 (in Appendix A). Because landsliding has previously occurred on this slope and it appears from the geomorphic analyses to be related to foliation in the Pelona Schist bedrock, we estimated the foliation dip from the stereo photo imagery and modeled a dipping foliation zone in the cross-section. Confining the upper part of the landslide to fail along this foliation zone, the slope stability software was used to search for the most likely location for the lower portion of the slip surface to form where it had to rupture across the rock foliation. A non-circular failure surface was used to accommodate this conceptual failure mode. Table 2 contains the material strength parameters used for LS-1 (A, B, and C). LS-1A under static conditions had a factor of safety of about 1.13, a low value that reflects its relatively unstable appearance.

Table 2. Material properties used in the stability and displacement analyses for landslides LS-1A, 1B and 1C.

Material	Angle of Internal Friction (degrees)	Cohesion (kN/m^3(pcf))
Intact Pelona Schist	45	33.5 (700)
Weathered Pelona Schist – intermediate depth landslide debris	40	33.5 (700)
Weathered Pelona Schist – shallow depth landslide debris	35	24 (152)
Alluvium	35	0
Pelona Schist deep foliation zone of weakness	25	33.5 (700)
Pelona Schist shallow foliation zone of weakness	25	14.4 (300)

Following the static analysis, the slope stability software was used to determine the seismic coefficient. This was done by iteratively applying horizontal coefficients until the factor of safety equaled one. Figure A2 shows the results of that evaluation. The seismic coefficient for LS-1A is 0.08g, and the average thickness of the landslide is 25 meters.

LS-1A Displacement Calculations:
LS-1A Input data:
Yield Acceleration = 0.08g
Average Thickness of Sliding Mass = 25m
Shear Wave Velocity of Sliding Mass = 385m/sec
Scenario Earthquake Magnitude (Mw) = 7.8
Site Peak Ground Acceleration (from PSHA) = 1.106g
Initial Fundamental Period of Sliding Mass = 0.26sec
Spectral Acceleration at Degraded Fundamental Period = 1.66g

Results:
Probability that Newmark Displacements are < 1cm = 0%
DISPLACEMENTS

Median Value	113cm
Minus 1 Sigma	**58cm**
Plus 1 Sigma	**218cm**

LS-1B Analysis**:** As was done for LS-1A, a foliation zone of weakness was projected from the main scarp into the subsurface and the slope stability software used this to constrain the upper part of the landslide. The lower portion of the landslide was more loosely constrained and the program searched for the critical surface across the rock foliation. This formed the plane for the middle part of the slide mass, which because it was landslide material, had a lower strength than intact Pelona Schist but slightly higher than LS-1A. LS-1B under static conditions had a factor of safety of about 1.26. The search for the seismic coefficient with the static slope stability configuration resulted in a value of 0.125g as shown in Figure A4.

LS-1B Displacement Calculations:
LS-1B Input data:
Yield Acceleration = 0.125g
Average Thickness of Sliding Mass = 30m
Shear Wave Velocity of Sliding Mass = 550m/sec
Scenario Earthquake Magnitude (Mw) = 7.8
Site Peak Ground Acceleration (from PSHA) = 1.106g
Initial Fundamental Period of Sliding Mass = 0.22sec
Spectral Acceleration at Degraded Fundamental Period = 1.66g

Results:
Based on Bray and Travasarou (2007) –
Probability that Newmark Displacements are < 1cm = 0%

DISPLACEMENTS All Site Conditions
Median Value 68cm
Minus 1 Sigma **35cm**
Plus 1 Sigma **131cm**

LS-1C Analysis: The same approach as used for landslides LS-1A and LS-1B was applied to LS-1C and the profiles are in Appendix A as Figures A5 and A6. The static factor of safety for LS-1C was about 1.50, a value which is representative of a more stable condition than LS-1A and LS-1B.

LS-1C Displacement Calculations:
LS-1C Input data:
Yield Acceleration = 0.21g
Average Thickness of Sliding Mass = 65m
Shear Wave Velocity of Sliding Mass = 770m/sec
Scenario Earthquake Magnitude (Mw) = 7.8
Site Peak Ground Acceleration (from PSHA) = 1.106g
Initial Fundamental Period of Sliding Mass = 0.34sec
Spectral Acceleration at Degraded Fundamental Period = 1.65g

Results:
Based on Bray and Travasarou (2007) –
Probability that Newmark Displacements are < 1cm = 0%
DISPLACEMENTS All Site Conditions
Median Value 41cm
Minus 1 Sigma **21cm**
Plus 1 Sigma **79cm**

Potential Lifelines Impacted: There are potentially five lifelines that could be impacted by failure of LS-1A, B, and C (listed in order of close proximity to landslide; Figure 3):

1) Two support towers for overhead transmission lines cross the central portion of the landslide,
2) One railway crosses the toe of the landslide,
3) Buried 36-inch gas pipeline passes less than 20 meters east of the base of the landslide,
4) A second railway passes within 100 meters east of the landslide toe,
5) Underground fiber-optic cable likely crosses somewhere between the second railway and the toe of the landslide.

*Scenario Earthquake Landslide Damage***:** Due to the recency of sliding, the shallow ground water table evidenced by seepage at the toe, the adversely dipping geology, and the high Newmark displacements (greater than two meters), LS-1 could fail catastrophically, especially the more recent portions of the slide mass, LS-1A and 1B. Figure 4 shows the lifelines and portions of lifelines that would be impacted by landslides.

If complete failure of LS-1A and 1B were to happen, the following damage would likely occur:

1) The two overhead transmission towers located on LS-1A would move downslope with the landslide and likely lose foundational support and collapse. Therefore, these towers would not be operational after the earthquake.
2) A 400-meter section of railway closest to the base of the slope would be undercut and displaced laterally more than ten meters to the northeast. This section of the railway could also be buried with up to five-million cubic yards of landslide debris. Damage of this magnitude would make this section of railway inoperable.
3) The buried 36-inch gas pipeline that passes within 20 meters east of the landslide could be displaced several meters laterally. In addition to possible disruption by lateral movement, the pipeline could also be covered by up to five-million cubic meters of landslide debris from LS-1A and 1B.
4) Because the second railway is over 100 meters away from the toe of the landslide, it is unlikely to be disrupted by this landslide. However, debris from the landslide could bury portions of this railway.
5) Because the location of the buried fiber optics cable is not known, it is unclear whether it will be damaged by failure of this landslide. If the fiber optics cable is buried within about 50 meters of the toe of the LS-1A, it might be displaced laterally and/or buried by the landslide.

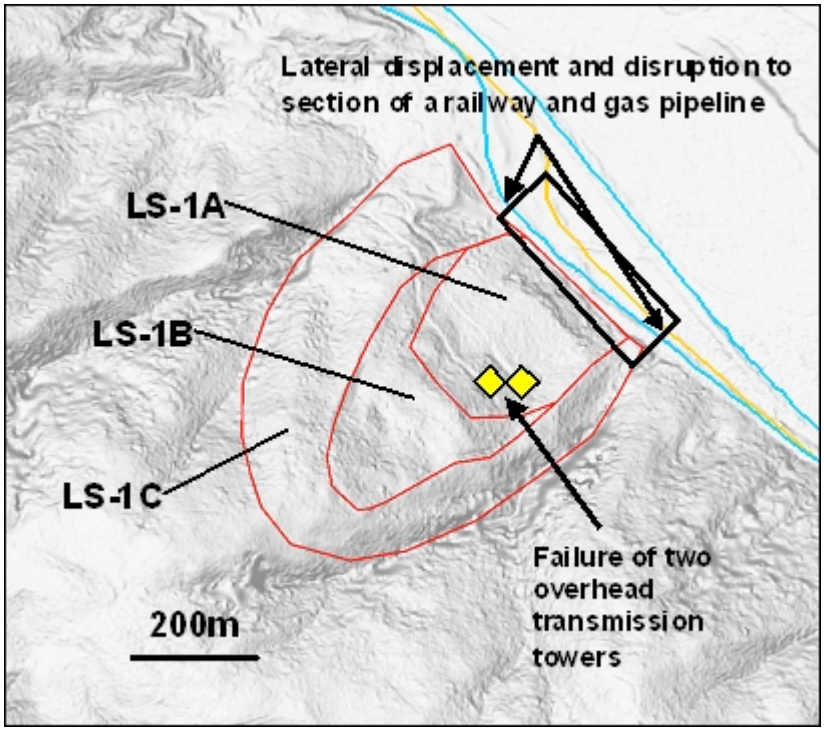

Figure 4. Parts A, B, and C of Cajon Pass focus area Landslide LS-1 observed on a shaded relief terrain image. Lifelines and portions of lifelines that are likely to be damaged by failure of this landslide are noted on the figure.

Landslide LS-2

Location: LS-2 is the basal portion of large landslide complex mapped by Morton and Miller (2006) located in the western section of the focus area, across the canyon from the Blue Cut (Figure 5).

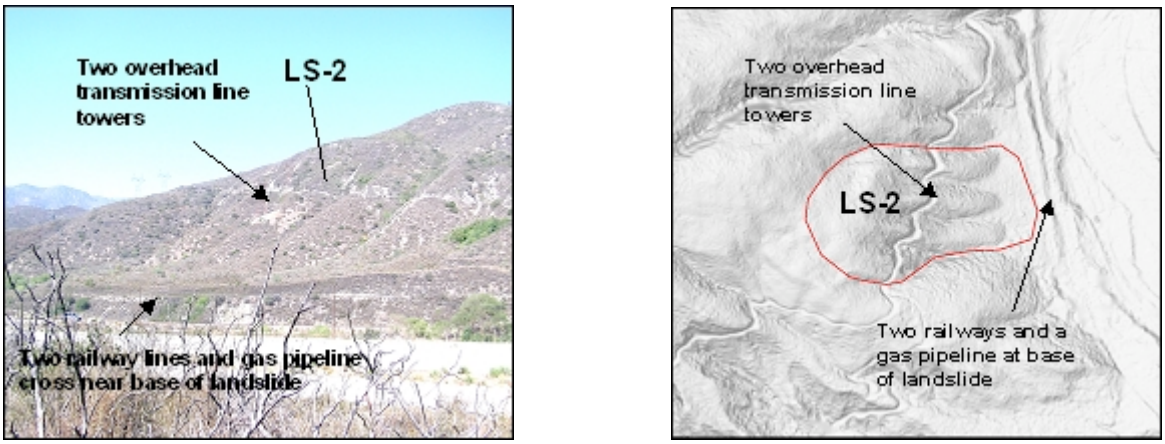

(a) (b)

Figure 5. Landslide LS-2 shown in (a) oblique view from across Cajon Canyon and (b) vertical view in shaded relief topography.

Notable Physical Features:

- large, older landslide that is deeply incised in the mid and lower slopes;
- arcuate headscarp and side scarps, and large bench;
- surface material appears highly weathered compared to surrounding rocks;
- foliation within outcrops of the Pelona Schist to the north is dipping about 20^{o} to the east, coinciding with the direction of sliding;
- age of slide may be inferred as very old, based on alluvial terrace deposit of probable Pleistocene age appearing to be partially deposited onto the toe of the slide.

Assumptions for Landslide Stability and Displacement Analyses: Based on the instability within the landslide complex, the following assumptions regarding the subsurface conditions were formulated:

1) The prospective location of the top of the landslide was bracketed based on the location of the headscarp.
2) The location of the base of reactivation of this landslide could pop-up underneath the alluvial terrace deposits that cover the toe. For this reason, the base of the modeled landslide was bracketed downslope within the terrace deposits.
3) Though there are likely weaker structural discontinuities within the slide mass, a moderate friction angle of 30^{o} was applied to the entire landslide mass as to best represent older landslide material.

4) A circular failure plane was applied to the landslide model to represent reactivated landslide material. In addition, the shallow dip (< 20°) of adjacent foliation within the Pelona Schist would likely have the same effect as a circular failure if relic foliation exists within the slide mass.

Table 3. Material properties used in the stability and displacement analyses for LS-2.

Material	Angle of Internal Friction (degrees)	Cohesion (kN/m^3(pcf))
Weathered Pelona Schist – intermediate depth landslide debris	30	33.5 (700)

LS-2 Analysis: The landslide profiles for LS-2 are in Appendix A as Figures A7 and A8. The static factor of safety for LS-2 was about 1.37.

LS-2 Displacement Calculations:

LS-2 Input data:

Yield Acceleration = 0.14g
Average Thickness of Sliding Mass = 30m
Shear Wave Velocity of Sliding Mass = 550m/sec
Scenario Earthquake Magnitude (Mw) = 7.8
Site Peak Ground Acceleration (from PSHA) = 1.076g
Initial Fundamental Period of Sliding Mass = 0.22sec
Spectral Acceleration at Degraded Fundamental Period = 1.55g

Results:

Probability that Newmark Displacements are < 1cm = 0%
DISPLACEMENTS

Median Value	61cm
Minus 1 Sigma	**31cm**
Plus 1 Sigma	**117cm**

Potential Lifelines Impacted: There are four potential lifelines that could be impacted by failure of LS-2 (Figure 5):

1) Two support towers for overhead transmission lines cross the central portion of the landslide,
2) A buried 36-inch gas pipeline passes within ten meters east of the base of the landslide,
3) One railway passes within 60 meters of the toe of the landslide,
4) A second railway passes within 125 meters east of the landslide toe.

Scenario Earthquake Landslide Damage: Due to the increased unstable condition, the adversely dipping geology, and the moderately high estimates of Newmark displacements (31 to 117 cm),

Landslide LS-2 could have catastrophic failure. Figure 6 shows the lifelines and portions of lifelines that would be impacted by landslides.

If complete failure of LS-2 were to happen, the following damage would likely occur:

1) The two overhead transmission line towers located on LS-2 would move downslope with the landslide and likely lose foundational support and collapse. Therefore, these towers will not be operational after the earthquake.
2) The buried 36-inch gas pipeline that passes within ten-meters east of the landslide could be displaced several meters laterally. In addition, the pipeline could be covered by up to 4.6-million cubic meters of landslide debris from LS-2.
3) A 400-meter section of the railway approximately 60 meters from the base of LS-2 could be undercut and displaced laterally several meters to the east. This section of the railway could also be buried up to 4.6-million cubic meters of landslide debris. Damage of this magnitude would make this section of railway inoperable.
4) Because the second railway is over 125 meters away from the toe of the landslide, it is unlikely to be disrupted by this landslide. However, there is a small chance that debris from the landslide could bury portions of this railway if it disaggregates into a flow failure.

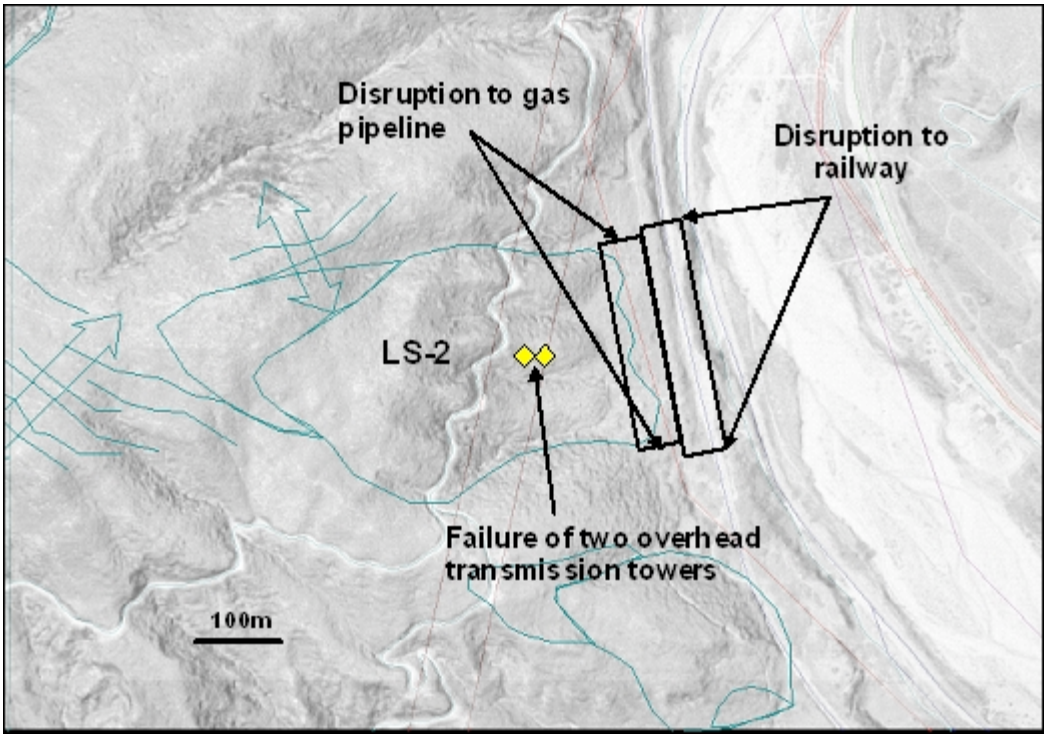

Figure 6. Cajon Pass focus area Landslide LS-2 observed on a shaded relief terrain image. Lifelines and portions of lifelines that are likely to be damaged by failure of this landslide are noted on the figure.

Landslide LS-3

Location: LS-3 is a small landslide mapped by Treiman (this study) in the northern part of the focus area, east of drainage and north of the San Andreas Fault (Figure 7).

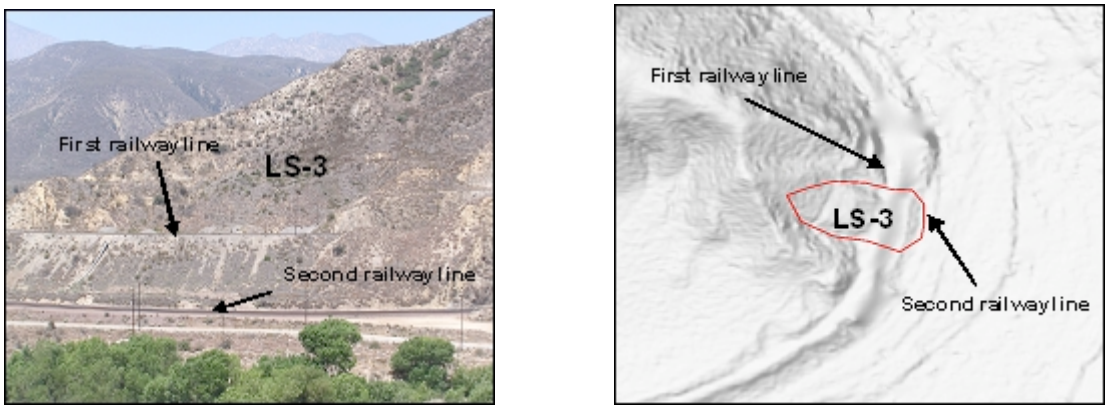

(a) (b)

Figure 7. Landslide LS-3 shown in (a) oblique view from across Cajon Canyon and (b) vertical view in shaded relief topography.

Notable Physical Features:

- small, relatively recent landslide;
- arcuate headscarp and side scarps well exposed;
- surface material appears to be highly weathered granodioritic rock;
- large amount of railway fill has been placed along the base of the landslide.

Assumptions for Landslide Displacement Analysis: Based on the instability within the landslide complex, the following assumptions regarding the subsurface conditions were formulated:

1) The prospective location of the top of the landslide was bracketed based on the location of the headscarp.
2) The location of the base of reactivation of this landslide could pop-up underneath the railway fill that cover the lower portion of the slide. For this reason, the base of the modeled landslide was bracketed downslope to the southeast of the fill.
3) Due to the relatively young age of this landslide mass, a friction angle of 28^{o} was applied as the strength of the slide material.

Table 4. Material properties used in the stability and displacement analyses for LS-3.

Material	Angle of Internal Friction (degrees)	Cohesion (kN/m^3(pcf))
Weathered – intermediate depth landslide debris	25	33.5 (700)

LS-3 Analysis: The landslide profiles for LS-3 are in Appendix A as Figures A9 and A10. The static factor of safety for LS-3 was about 1.83.

LS-3 Displacement Calculations:

LS-3 Input data:

Yield Acceleration = 0.28g
Average Thickness of Sliding Mass = 10m
Shear Wave Velocity of Sliding Mass = 385m/sec
Scenario Earthquake Magnitude (Mw) = 7.8
Site Peak Ground Acceleration (from PSHA) = 1.097g
Initial Fundamental Period of Sliding Mass = 0.104sec
Spectral Acceleration at Degraded Fundamental Period = 2.14g

Results:

Probability that Newmark Displacements are < 1cm = 0%
DISPLACEMENTS

Median Value	15cm
Minus 1 Sigma	8cm
Plus 1 Sigma	29cm

Potential Lifelines Impacted: There are three potential lifelines that could be impacted by failure of LS-3 (Figure 7):

1) One railway crosses the lower one-third of the landslide,
2) A second railway slightly crosses the toe of the landslide, and,
3) A buried fiber-optics cable may be in the vicinity of LS-3; the exact location of this cable is not known in the area.

Scenario Earthquake Landslide Damage: Due to the increased stability of the landslide from the placement of fill at its base, and the relatively low estimated Newmark displacements calculated (8 to 29 cm), LS-3 would not likely fail catastrophically. However, displacements of up to one-quarter meter could occur, possibly damaging the two railway lines that cross the base of the landslide. Figure 8 shows the lifelines and portions of lifelines that would be impacted by landslides.

If failure of LS-3 of one-quarter meter were to happen, the following damage would likely occur:

1) The 200-meter section of the railway that crosses the lower one-third of the landslide could be displaced and/or deflected by up to about 30 cm to the east, with the most significant deflections occurring along the north and south edges of the landslide. Some small portion of the existing slide material could also fail onto the track, causing blockage to that segment, but this is unlikely because this section of the railway is elevated.
2) The 200-meter section of the second railway that crosses near the base of the existing landslide could also be deflected up to 30 cm to the east. Debris falling onto this railway from upslope areas could also cause blockage.

3) Depending on the location of the buried fiber-optics cable, a large section of this utility could be displaced to the east. It is not clear whether 30 cm of displacement could cause significant damage to the fiber-optics cable.

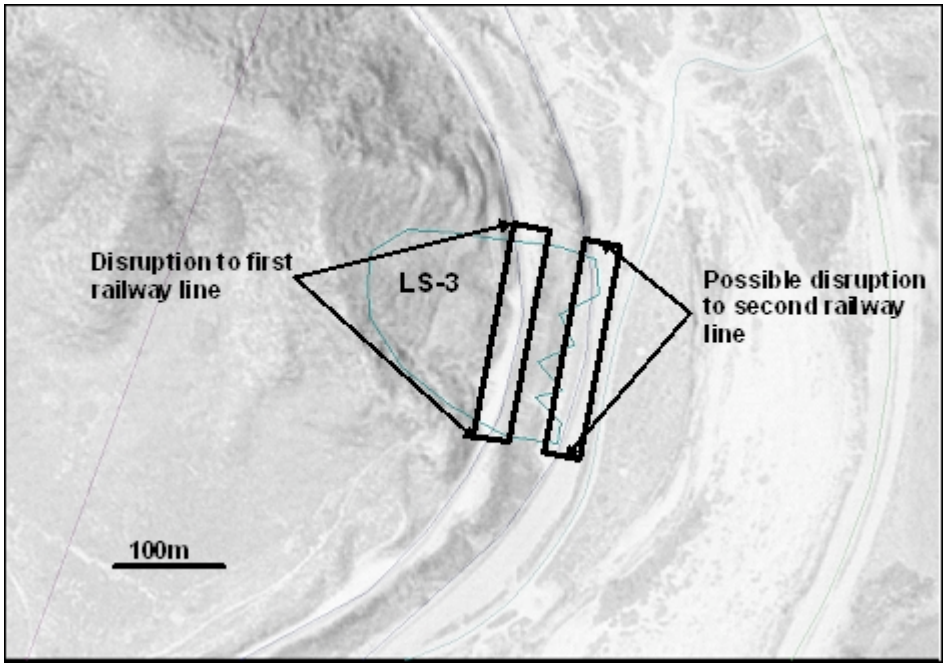

Figure 8. Cajon Pass focus area Landslide LS-3 observed on a shaded relief terrain image. Lifelines and portions of lifelines that are likely to be damaged by failure of this landslide are noted on the figure.

Landslide LS-4

Location: LS-4 is on a north-facing slope, south and across from the Blue Cut area, in the southern portion of the focus area (Figure 9).

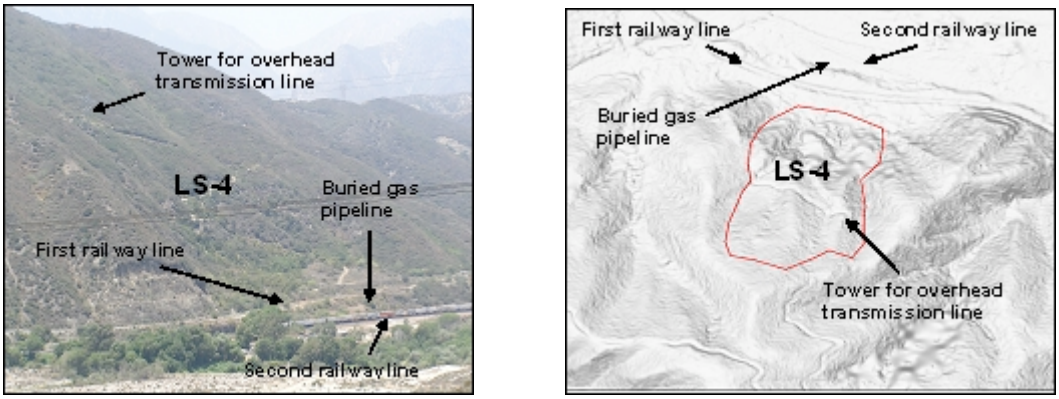

(a) (b)

Figure 9. Landslide LS-4 shown in (a) oblique view from across Cajon Canyon and (b) vertical view in shaded relief topography.

Notable Physical Features:

- relatively steep slopes around and within landslide mass;
- has similar appearance to and possibly as active as LS-1C;
- large headscarp area;
- side scarps funnel landslide mass towards bottom;
- the heavy vegetation in lower half of the landslide and especially at the base imply that ground water is relatively shallow within the slide mass;
- according to Morton and Miller (2006), Pelona Schist foliation in the area dips to the west and southwest implying that foliation is not a factor in landsliding;
- based on the shape of the slide, it appears to be relatively shallow for its size.

Assumptions for Landslide Displacement Analysis: Based on the instability within the landslide complex, the following assumptions regarding the subsurface conditions were formulated:

1) The location of the prospective top of the landslide was bracketed based on the location of the headscarp.
2) Based on the shallow nature of the slide deposit, a shallow slide plane was applied to the model. The base of sliding was also placed at the base of the slope for this reason.
3) Due to the dense vegetation in the lower half of the slide mass, a ground-water table was placed within 25 meters of the ground surface.
4) Due to the relatively young age of this landslide mass, a friction angle of 28^{o} was applied as the strength of the slide material.

Table 5. Material properties used in the stability and displacement analyses for Landslide LS-4.

Material	Angle of Internal Friction (degrees)	Cohesion (kN/m^3(pcf))
Weathered Pelona Schist – intermediate depth landslide debris	28	33.5 (700)

LS-4 Analysis: The landslide profiles for LS-4 are in Appendix A as Figures A11 and A12. The static factor of safety for LS-4 was about 1.13, which reflects the young and tenuous stability of this landslide.

LS-4 Displacement Calculations

LS-4 Input data:

Yield Acceleration = 0.04g
Average Thickness of Sliding Mass = 25m
Shear Wave Velocity of Sliding Mass = 385m/sec
Scenario Earthquake Magnitude (Mw) = 7.8
Site Peak Ground Acceleration (from PSHA) = 1.101g
Initial Fundamental Period of Sliding Mass = 0.26sec
Spectral Acceleration at Degraded Fundamental Period = 1.72g

Results:

Based on Bray and Travasarou (2007) –
Probability that Newmark Displacements are < 1cm = 0%
DISPLACEMENTS

Median Value	166cm
Minus 1 Sigma	86cm
Plus 1 Sigma	321cm

Potential Lifelines Impacted: There are four potential lifelines that could be impacted by failure of LS-3 (Figure 9):

1) An overhead transmission line tower lies within the eastern portion of the landslide,
2) The first railway passes within about ten meters of the toe of the landslide,
3) A buried 36-inch gas pipeline passes within 40 meters north of the base of the landslide,
4) The second railway passes within 100 meters north of the landslide toe.

Scenario Earthquake Landslide Damage: Due to the recency of sliding, the shallow ground water, and the high estimated Newmark displacements calculated (greater than three meters), Landslide LS-4 could fail catastrophically. Figure 10 shows the lifelines and portions of lifelines that would be impacted by landslides.

If complete failure of LS-4 were to happen, the following damage would likely occur:

1) The overhead transmission towers located in the upper portion of the landslide would move downslope with the landslide and likely lose foundational support and collapse. Therefore, this tower will not be operational after the earthquake.
2) A 400-meter section of the railway that crosses near the base of LS-4 could be buried under approximately 2.5-million cubic meters of landslide debris. Damage of this magnitude would make this section of railway inoperable.
3) Although less likely to happen, a 250-meter section of both the second railway and buried 36-inch gas pipeline could be covered by landslide debris.

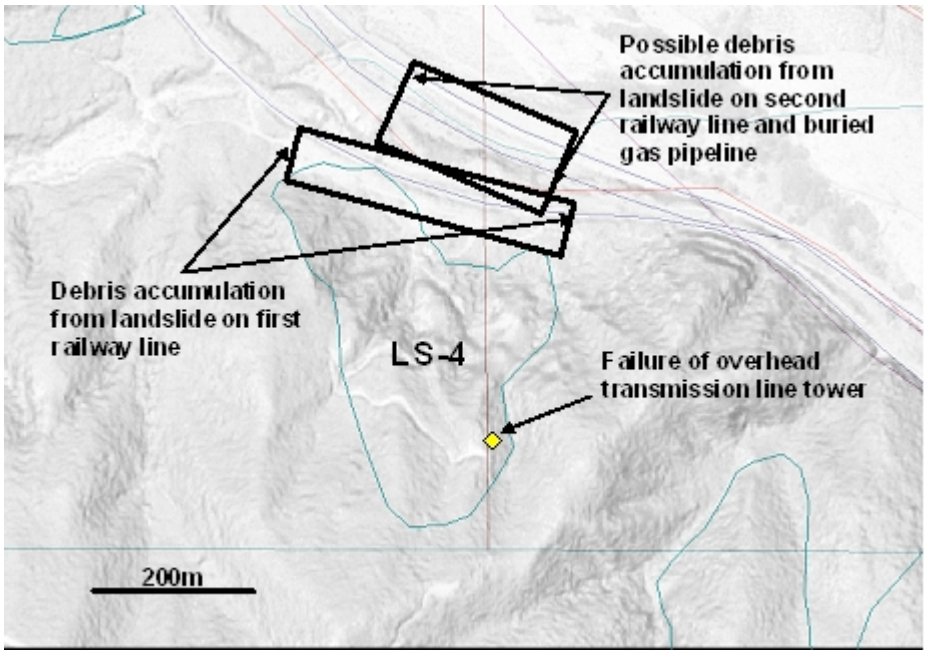

Figure 10. Cajon Pass focus area Landslide LS-4 observed on a shaded relief terrain image. Lifelines and portions of lifelines that are likely to be damaged by failure of this landslide are noted on the figure.

Landslide LS-5

Location: LS-5 is a moderate-sized landslide mapped by Treiman (this study) located just north of the focus area boundary, originating east of and underlying Interstate 15 (Figure 11).

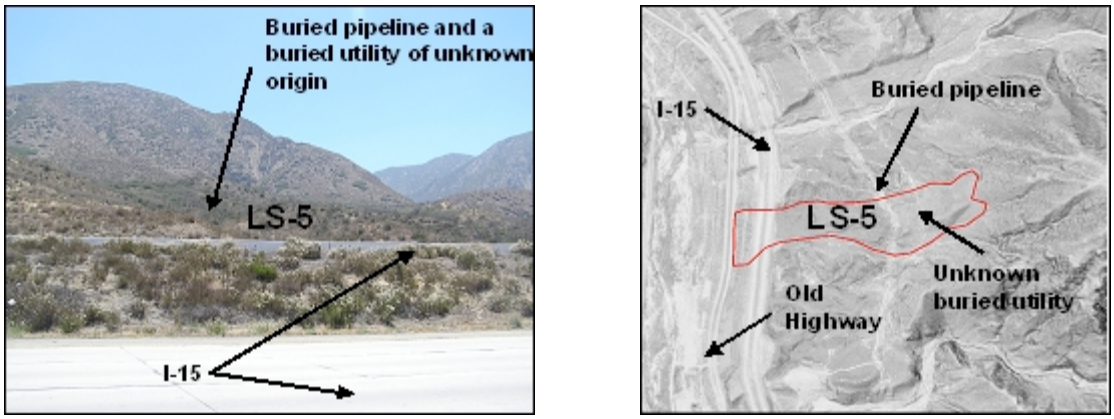

(a) (b)

Figure 11. Landslide LS-5 shown in (a) oblique view from across Cajon Canyon and (b) vertical view on a DOQQ with shaded relief topography.

Notable Physical Features:

- landslide is elongate in shape;
- hummocky topography throughout slide mass;
- part of the central section of the slide has been eroded and bedrock has been exposed;
- toe of slide is covered by moderate amount of highway road fill;
- terrain is steeper in the upper portion of the slide mass than in the lower half.

Assumptions for Landslide Displacement Analysis: Based on the instability within the landslide complex, the following assumptions regarding the subsurface conditions were formulated:

1) Because of the low relief of the lower half and the resisting forces provided by the highway fill, only the upper portion of the slide mass was evaluated for potential failure.
2) The prospective location of the top of the landslide was bracketed based on the location of the upper part of the slide mass.
3) A low friction angle of 25^{o} was applied to the entire landslide due to the redistribution and, therefore, weakening of material within the slide material.

Table 6. Material properties used in the stability and displacement analyses for Landslide LS-5.

Material	Angle of Internal Friction (degrees)	Cohesion (kN/m^3(pcf))
Weathered Cajon Valley Formation, Unit 5 – intermediate depth landslide debris	25	33.5 (700)

LS-5 Analysis: The landslide profiles for LS-5 are in Appendix A as Figures A13 and A14. The static factor of safety for LS-5 was about 2.09.

LS-5 Displacement Calculations:

LS-5 Input data:

Yield Acceleration = 0.35g
Average Thickness of Sliding Mass = 25m
Shear Wave Velocity of Sliding Mass = 770m/sec
Scenario Earthquake Magnitude (Mw) = 7.8
Site Peak Ground Acceleration (from PSHA) = 1.10g
Initial Fundamental Period of Sliding Mass = 0.26sec
Spectral Acceleration at Degraded Fundamental Period = 1.93g

Results:

Based on Bray and Travasarou (2007) –
Probability that Newmark Displacements are < 1cm = 0%
DISPLACEMENTS

Median Value	14cm
Minus 1 Sigma	7cm
Plus 1 Sigma	28cm

Potential Lifelines Impacted: There are three potential lifelines that could be impacted by failure of LS-5 (Figure 11):

1) A buried petroleum pipeline crosses the central portion of the landslide,
2) Another buried utility of unknown use crosses the central portion of the landslide, and,
3) I-15 crosses the toe of the landslide and the Old Highway (old Route 66).

Scenario Earthquake Landslide Damage: Because of the low relief of the lower half and the slide resisting force provided by the highway fill, only the upper portion of the slide mass was evaluated for potential failure (Figure 12). The location of the top of the speculative landslide was bracketed based on the location of the upper, steeper part of the slide mass.

Because this portion of the landslide had a relatively low estimated Newmark displacements (six to 27 cm), LS-5 is not likely to fail catastrophically. However, displacements of up to one-

quarter meter could occur, possibly causing damage to the two utilities that cross the upper portion of the landslide. Figure 12 shows the lifelines and portions of lifelines that would be impacted by landslides.

If failure of LS-5 of one-quarter meter were to happen, the following damage would likely occur:

1) The 200-meter section of the pipeline that crosses the upper part of LS-5 could be displaced and/or deflected up to about 30 cm to the west, with the most significant deflections occurring along the north and south edges of the landslide.
2) As with the pipeline above, the 200-meter section of the unknown buried utility that crosses the same portion of the landslide could also be deflected by up to about 30 cm to the west.
3) Neither I-15 or the Old Highway are likely to be affected by the portion of LS-5 expected to move.

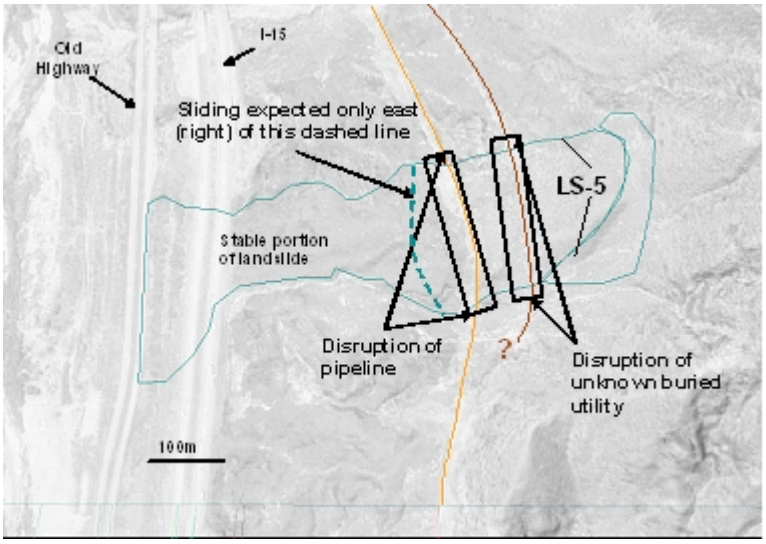

Figure 12. Cajon Pass focus area Landslide LS-5 observed on a shaded relief terrain image. Lifelines and portions of lifelines that are likely to be damaged by failure of this landslide are noted on the figure.

Shallow Landslide Analysis

Landslide Hazard Potential Map

As part of the MHDP, CGS geologists prepared a seismically induced landslide hazard potential map of the Cajon Pass focus area to identify areas more likely to experience relatively shallow slope failure during the scenario earthquake.

The methodology used to make this map is utilized by CGS to produce earthquake-induced landslide hazard zones and is based on earthquake ground-shaking estimates, geologic material-strength estimates, and slope gradient. These data are gathered from a variety of outside sources. Digital terrain data from a photogrammetric (ISTAR), two-meter digital elevation model (DEM) was used in this evaluation. Geologic mapping from Morton and Miller (2006) was used to provide the spatial distribution of geologic materials in the study area. In addition, a map of existing landslides by Treiman (this study) provided an update of the landslide inventory in the study area. Geologic units were grouped together by relative material (rock) strength for the analysis (Figure 13).

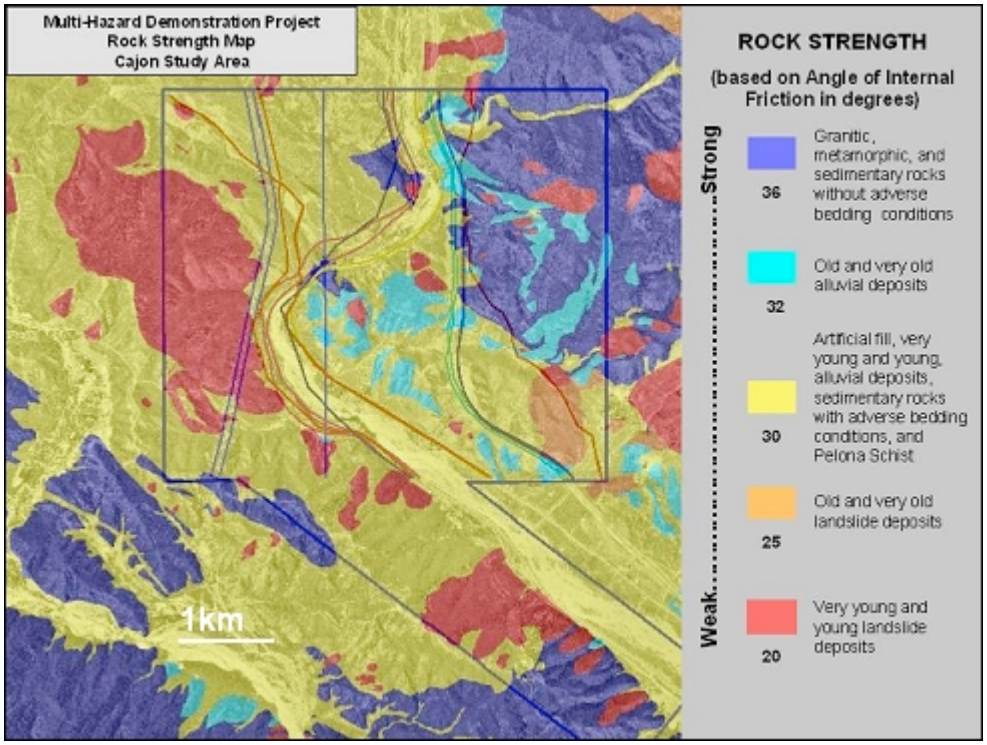

Figure 13. Map showing material (rock) strength for groups of geologic units in the Cajon Pass focus area. Strength is categorized based on the estimated "Angle of Internal Friction" for each group of geologic units.

The data collected for this evaluation were processed into GIS layers and a slope stability analysis was performed using the Newmark method of analysis (Newmark, 1965), resulting in a map of landslide hazard potential. Landslide hazard potential is categorized by the following

Newmark displacement amounts: "very low" for displacements less than 5 cm, "low" for displacements between 5 cm and 15 cm, "moderate" for displacements between 15 cm and 30 cm, and "high" for displacements above 30 cm.

Ground Motions and Newmark Analysis - To evaluate earthquake-induced landslide hazard potential in the study area, a method of dynamic slope stability analysis developed by Newmark (1965) was used. The Newmark method analyzes dynamic slope stability by calculating the cumulative down-slope displacement for a given earthquake strong-motion time history. As implemented for the preparation of earthquake-induced landslide zones, the Newmark method necessitates the selection of a design earthquake strong-motion record to provide the "ground shaking opportunity."

The strong-motion record selected for this analysis is the Southern California Edison (SCE) Lucerne record from the 1992 magnitude 7.3 Landers, California, earthquake. This record has a source to recording site distance of 1.1 km and a peak ground acceleration (PGA) of 0.80g. Although smaller than the scenario earthquake, this record is the largest available to CGS at this time.

The design strong-motion record was used to develop a relationship between landslide displacement and yield acceleration (a_y), defined as the earthquake horizontal ground acceleration above which landslide displacements take place. This relationship was prepared by integrating the design strong-motion record twice for a given acceleration value to find the corresponding displacement, and the process was repeated for a range of acceleration values (Jibson, 1993).

Displacements of 30, 15 and 5 cm are used as criteria for rating levels of earthquake-induced landslide hazard potential based on the work of Youd (1980), Wilson and Keefer (1983), and the CGS pilot study for earthquake-induced landslides (McCrink and Real, 1996). These displacements correspond to yield accelerations of 0.148, 0.182, and 0.243g.

Slope Stability Analysis - A slope stability analysis was performed for each geologic material strength group at slope increments of one degree. An infinite-slope failure model under unsaturated slope conditions was assumed. A factor of safety was calculated first, followed by calculation of yield acceleration from Newmark's equation:

$$a_y = (FS - 1)g \sin \alpha$$

where FS is the Factor of Safety, g is the acceleration due to gravity, and α is the direction of movement of the slide mass, in degrees measured from the horizontal, when displacement is initiated (Newmark, 1965). For an infinite slope failure, α is the same as the slope angle.

The yield accelerations resulting from Newmark's equations represent the susceptibility to earthquake-induced failure of each geologic material strength group for a range of slope gradients. Based on the relationship between yield acceleration and Newmark displacement shown in Figure 14, hazard potentials were assigned as follows:

1. If the calculated yield acceleration was less than 0.142g, Newmark displacement greater than

30 cm is indicated, and a HIGH hazard potential was assigned.

2. Likewise, if the calculated yield acceleration fell between 0.142g and 0.183g, Newmark displacement between 15 cm and 30 cm is indicated, and a MODERATE hazard potential was assigned.
3. If the calculated yield acceleration fell between 0.183g and 0.243g, Newmark displacement between 5 cm and 15 cm is indicated, and a LOW hazard potential was assigned.
4. If the calculated yield acceleration was greater than 0.243g, Newmark displacement of less than 5 cm is indicated, and a VERY LOW potential was assigned.

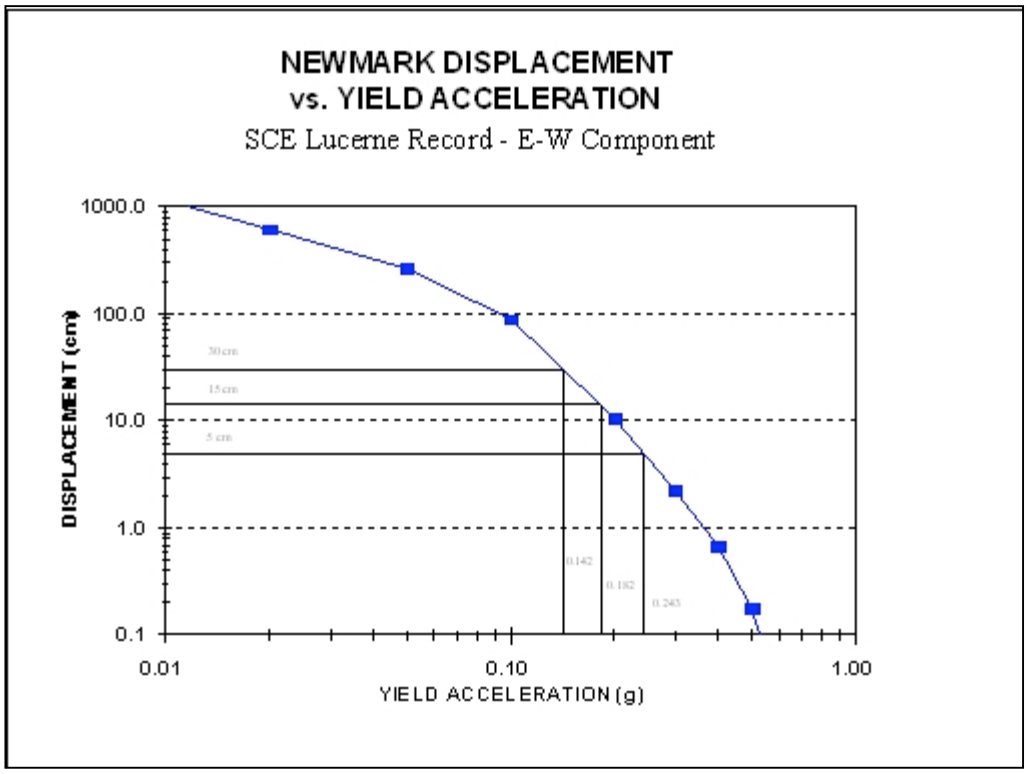

Figure 14: Yield Acceleration vs. Newmark Displacement for the Southern California Edison Lucerne Record from the 1992 magnitude 7.3 Landers earthquake.

The earthquake-induced landslide, hazard potential map was prepared by combining the geologic material-strength values and the average slope according to this equation (Figure 15). The portions of the map circled and labeled as "Areas of Concern" are where shallow landslides have the greatest chance to affect the numerous lifelines that cross the area.

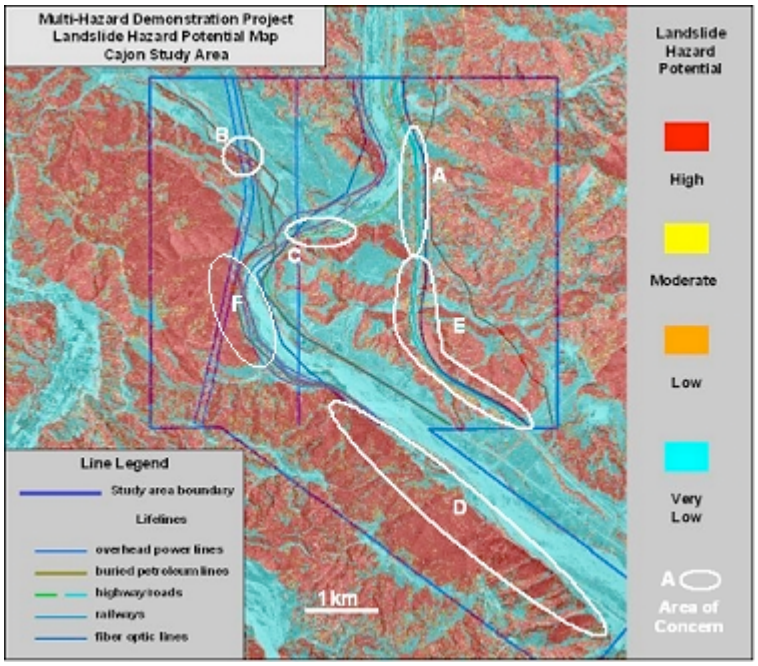

Figure 15. Landslide hazard potential map for the Cajon Pass focus area.

Shallow Landslide Areas

CGS has identified at least six areas where lifelines cross slopes with high hazard potential for shallow landslides to occur during a large earthquake. These are areas where shallow landslides are likely to cause the most significant impact to transportation and utility lifelines in the Cajon Pass focus area. A more comprehensive analysis was performed in Areas C and E where detailed landslide debris amounts were calculated at the request of the USGS and Caltrans.

The shallow landslide areas of concern are discussed below:

Area A: The large artificial fill prisms constructed for I-15 will likely have seismic compression/settlement and possibly landslide failures during a very large earthquake. There is evidence from numerous earthquakes that seismic compression and/or vertical settlement occurs on large highway fill prisms such as the one through Cajon Pass (Figure 16). However, it is more difficult to evaluate the lateral (landslide) stability of these materials and slopes considering such a large earthquake event, like the one in this evaluation. Sufficient data is not available to analyze the stability of large highway fill prisms during long-duration, high ground motion (+1g) events.

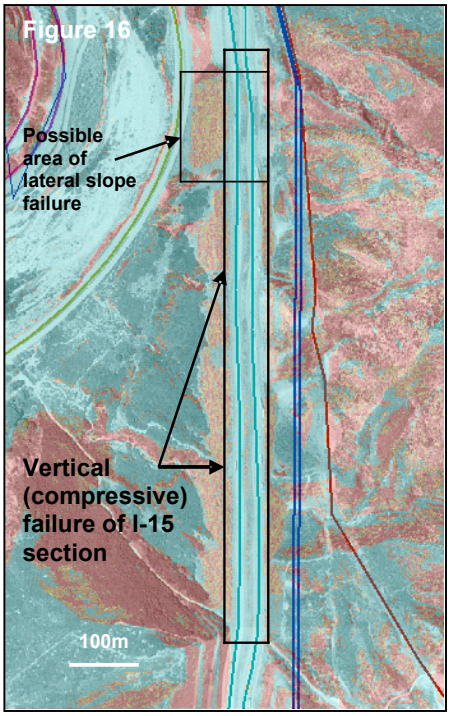

Scenario Earthquake Landslide Damage: The large highway fill prisms will likely have a significant amount of seismically induced settlement, with cracks potentially displacing the highway up to several meters vertically. In addition, considering the long duration of high ground motions expected, a scenario could include a large portion of the highway fill prism failing catastrophically in a westerly direction and that a significant section of both the north and south bound lanes would be displaced significantly. This is most likely to occur in the northern portion of the fill prism where the slope is the longest (Figure 17 below). Failure of this fill prism could also deposit a significant amount of material on the Old Highway.

Area B: Older alluvial terrace deposits and landslide-prone Pelona Schist that have been deeply incised, specifically in the area where Lone Pine and Cajon Canyons come together, could fail causing damage to adjacent overhead transmission line towers and pipelines that cross these slopes (Figure 18). The hazard potential map (Figure 15) indicates that there is a high potential for shallow sliding on these slopes in a number of places.

Scenario Earthquake Landslide Damage: As shown in Figure 19 below, a damage scenario would involve disruption and/or failure of several utility lifelines. The set of overhead power-line towers (Figure 18), which are within two to three meters of the top edge of the slope, could fail into the adjacent canyon with this slope during the scenario earthquake. In addition, several buried petroleum product lines that either cross or have been placed along the top of the steep south-facing slope, could be disrupted in a number of places if these slopes fail. Displacement of these utilities could be on the order of five to 50 meters, depending on height of the slope on which they are located.

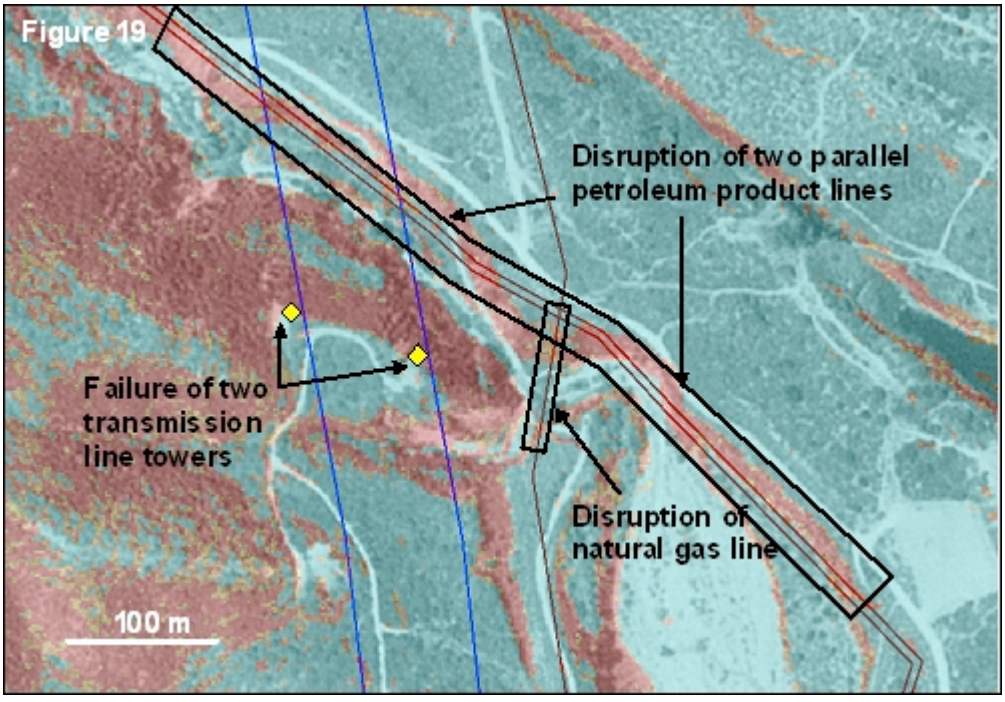

Area C and E (Highways): As discussed previously, a more comprehensive analysis was performed to estimate the impacts from shallow landslides within road cuts (Areas C and E), as well as the erosional undercutting beneath the Old Highway (Area C), in the Cajon Pass focus

area. The road cuts have been separated into sections based on landslide hazard potential and additional information from our fieldwork and the geology of the area (Figures 20a and b).

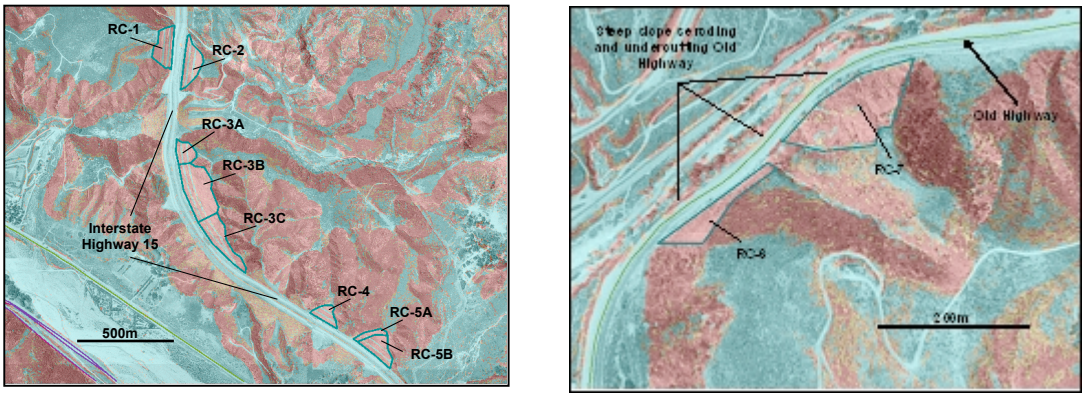

(a) (b)

Figure 20. Maps showing the location of the road cuts evaluated: (a) shows Area E, and (b) shows Area C. The colors represent the landslide hazard potential from Figure 15.

Each road-cut is ranked as a whole based on the results of a landslide hazard potential map created at the Cajon Pass focus area (Figure 15), as well as field data and other observations. The slopes in question have been classified as either having an overall “moderate” or “high” rating of hazard potential based on the amount of Newmark displacement that is anticipated. Slopes with "moderate" hazard potential average between 15 cm and 30 cm of Newmark displacement over the area of the slope, whereas the slopes with "high" hazard potential average over 30 cm of displacement.

There are several general characteristics for the road cuts in the Cajon Pass area: 1) due to their proximity to the San Andreas Fault, the material that make up their slopes is highly fractured and, therefore, will be on average made up of cobble-size material with boulders of one-cubic-meter possible but unlikely, 2) the Pelona Schist, a geologic unit prone to landslides, forms the majority of the road-cut slopes in the area, 3) the cut slopes along I-15 are 2:1 and contain numerous debris-collection benches, reducing the amount of debris that will be shed onto the highway, and 4) the cut slopes along the Old Highway have slopes greater than 2:1, have been in-place for a much longer time, do not appear to be extensively maintained and, therefore, are deeply eroded and failing in places.

The following is a discussion of the unique characteristics of each road-cut section and reasons why they were given their relative hazard potential rating:

Road-cut RC-1 (Area E): This east-facing road cut (Figure 21 right) is approximately 65-meters tall and located in northern part of Area E. This road cut was given a "high" hazard potential rating because: 1) foliation planes within the Pelona Schist dip out of slope, creating "adverse" conditions for sliding, and 2) because it is located directly adjacent to the San Andreas fault, the cut slope material is more heavily fractured than other road cuts in the area.


Figure 21

Road-cut RC-2 (Area E): Across from and facing RC-1, the west-facing RC-2 (Figure 22) is also 65-meters tall but was given a "moderate" hazard potential rating because, per area, the flat-lying benches make up a significant portion of the cut slope in plane-view. These "low" hazard bench areas offset the "high" hazard potential of the slopes, making the average hazard potential "moderate."


Figure 22

Road-cut RC-3A (Area E): This portion of road-cut RC-3 is approximately 60-meters tall and forms the northern end of this large road-cut. RC-3A was given a "high" hazard potential rating because sections of this slope contain small landslides (Figure 23). The geologic material that makes up this section appears to be weaker than the surrounding material.


Figure 23

Road-cut RC-3B (Area E): This central section of the RC-3 is the tallest (>100 meters) slope of any road-cut in the Cajon Canyon area (Figure 24). Due to the great height of this slope, and fewer debris catchment benches (two) proportional to that slope, this slope was given a "high" hazard potential rating overall.


Figure 24

Road-cut RC-3C (Area E): This portion of road-cut RC-3 is approximately 60-meter tall and forms the southern part of that road-cut (Figure 25). This slope area was given a "moderate" hazard potential rating because, per area, the flat-lying benches make up a significant portion of the cut slope in plane-view. These "low" hazard bench areas offset the "high" hazard potential of the slopes, making the average hazard potential "moderate."

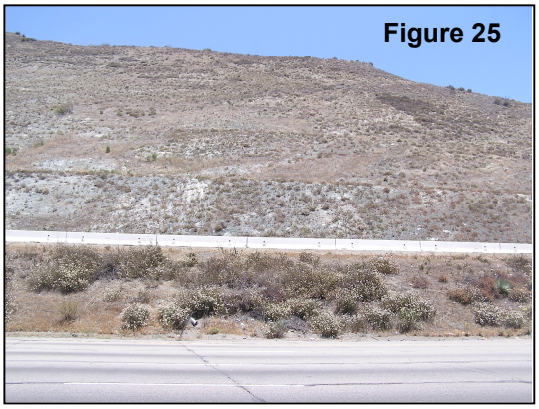
Figure 25

Road-cut RC-4 (Area E): This west-facing road-cut (Figure 26) is approximately 60-meters tall. RC-4 was given a "moderate" hazard potential rating because, per area, the flat-lying benches make up a significant portion of the cut slope in plane-view. These "low" hazard bench areas offset the "high" hazard potential of the slopes, making the average hazard potential "moderate."


Figure 26

Road-cut RC-5A (Area E): This portion of road-cut RC-5 is approximately 85-meters tall and forms the northern end of RC-5. It was given a "high" hazard potential rating because it is composed of old landslide material, as mapped by Morton and Miller (2006; shown in Figure 13) and identifiable by its lighter color (Figure 27). The geologic material that makes up this section is weaker than the surrounding material.

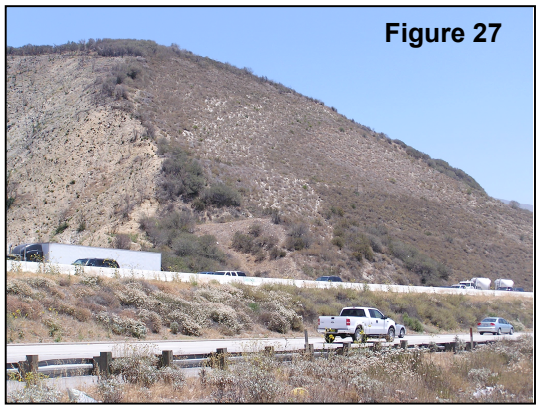
Figure 27

Road-cut RC-5B (Area E): The southern section of RC-5 is approximately 60-meters tall and was given a "moderate" hazard potential rating because, per area, the flat-lying benches make up a significant portion of the cut slope in plane-view. These "low" hazard bench areas offset the "high" hazard potential of the slopes, making the average hazard potential "moderate." This portion of the RC-5 is shown in Figure 27 as the darker portion of the slope to the right.

Road-cuts RC-6, RC-7, and the Slope Undercutting the Old Highway (Area C): The steep road-cuts above and the undercut slopes below the Old Highway are comprised of weak, heavily fractured and altered Pelona Schist (Figure 28). RC-6 is approximately 50-meters tall with a slope of 3/4:1 (133%). RC-7 is approximately 80-meters tall with a slope of 1.25:1 (80%). The slope undercutting the Old Highway is about 30-meters tall and has a slope of greater than 3/4:1 (>133%).

All three slopes are prone to slope failures and are already a source of damage to the road. The hazard is so severe that rockfall fences (Figure 29) and concrete barriers (Figure 30) currently protect the Old Highway. In the event of a large earthquake on the San Andreas Fault, these slopes could be susceptible to significant failure, causing considerable damage to the Old Highway. This damage might not only limit access to that road but also to other lifelines throughout the Cajon Pass corridor.

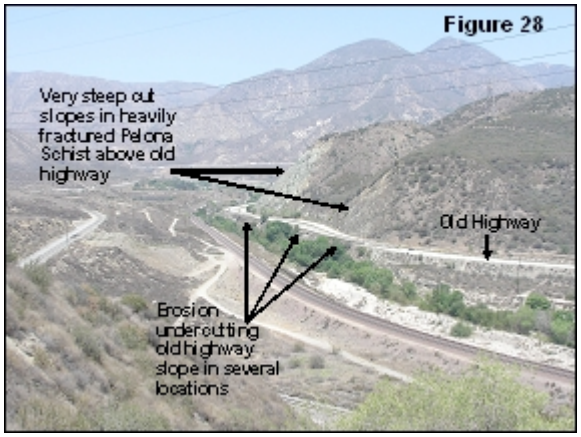

Figure 28

The severity of slope failure is so significant that these slopes are all given a "high" hazard potential rating.

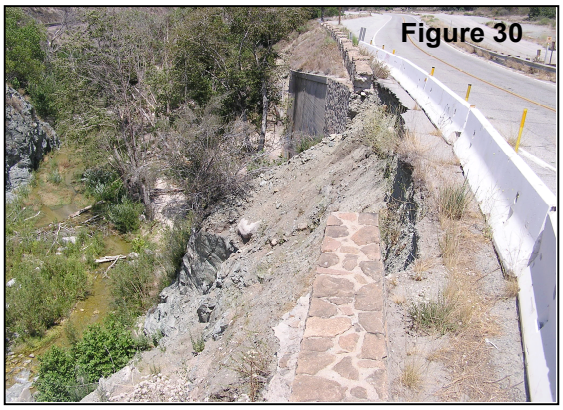

Scenario Earthquake Landslide Damage for Highways in Areas C and E: Upper-bound volume estimates of landslide debris materials that could fall on highways have been calculated for the Cajon Pass road-cuts discussed above. The calculations incorporated the planimetric area of each slope and a numerical representation of the different levels of hazard potential for the slopes.

The depth of slide material was determined based partly on hazard potential, as well as observations made in the field regarding the following conditions (road-cuts that exhibit negative impacts from these conditions are listed in parentheses): 1) the potential for failure from adversely dipping foliation and fractures (RC-1, RC-6, and RC-7), 2) the amount and density of the fractures within the rock (RC-1, RC-6, and RC-7), 3) the presence of existing slope failures or old landslide material (RC-3A, RC-5A, RC-6, and RC-7), 4) the degree to which the slope has been eroded or weathered (RC-6 and RC-7), and 5) the height of the cut-slope as it relates to the number of debris-catchment benches that cross the slope (RC-3B, RC-6, and RC-7). Slopes that were not negatively influenced by these factors and that had a "moderate" hazard potential ranking were calculated to have no more than one-meter depth of slide material. Slopes that were affected by up to two of these factors and given a "high" hazard potential ranking were calculated to have a potential landslide depth of two meters. Slopes that were affected by three or more of these factors were calculated to have a depth of three meters.

Jibson *et al.* (2000; 1998) developed a relationship between Newmark displacement and the percent chance that any cell in that displacement range will be occupied by an earthquake triggered landslide source. Extrapolating their relationship to represent the percentage of area failed for Newmark displacement ranges in the hazard potential map (Figure 15), we can estimate the area of each road cut affected by slope failure. In the case of this study, the road-cuts of "high" hazard potential, representing slopes with greater than 30 cm of Newmark displacement, were multiplied by 34%, which represents the area of that slope expected to fail. Road-cuts with "moderate" hazard potential were multiplied by 32% to represent the slope expected to fail on those slopes.

Table 7 contains conservative estimates of landslide debris volumes that could be deposited on I-15 and Old Highway in the Cajon Pass area. According to these calculations, the total high-end amount of debris to be shed on I-15 would be about 73,500 cubic-meters, and the total amount

for the Old Highway would be 16,500 cubic-meters. The Old Highway might also fail from the slope undercutting the road.

Table 7. Upper-Bound Debris Volume Estimates for Road-Cuts in the Cajon Pass Focus Area.

Highway Affected	**Road Cut Area**	Total Planimetric Area (sq-m)	Hazard Potential Designation	Thickness of Failure (m)	% Area Slope to Fail	**Volume of Material (cu-m)**	***Volume of Material (cu-yards)***
I-15	**RC-1**	18,455	High	2	34	**12,549**	***16,414***
	RC-2	18,691	Moderate	1	32	**5,981**	***7,823***
	RC-3A	10,892	High	2	34	**7,406**	***9,687***
	RC-3B	40,892	High	2	34	**27,807**	***36,372***
	RC-3C	25,941	Moderate	1	32	**8,301**	***10,858***
	RC-4	9,269	Moderate	1	32	**2,966**	***3,880***
	RC-5A	4,834	High	2	34	**3,287**	***4,299***
	RC-5B	16,426	Moderate	1	32	**5,256**	***6,875***
Old Hwy	**RC-6**	3,726	High	3	34	**3,801**	***4,971***
	RC-7	12,405	High	3	34	**12,653**	***16,550***

Area C (Non-Highway Lifelines): As discussed, steep, rockfall-prone road-cuts and slopes undercutting the Old Highway comprised of weak, heavily fractured and altered Pelona Schist around the area of the Blue Cut are already a source of damage to the road. The hazard is so severe that rockfall fences and concrete barriers are presently in place to protect the Old Highway. However, in the event of a large earthquake, these slopes could be susceptible to permanent failure of the Old Highway, not only limiting access to that road but to other lifelines throughout the Cajon Pass corridor. In addition to the road, there are two other utility lifelines that may be affected (Figure 31). A single overhead transmission line tower is situated at the top edge of a steep, side-canyon slope that is considered to have a high-hazard potential. In addition, a high hazard potential exists where a fiber-optics communication line crosses the erosional slope beneath the Old Highway.

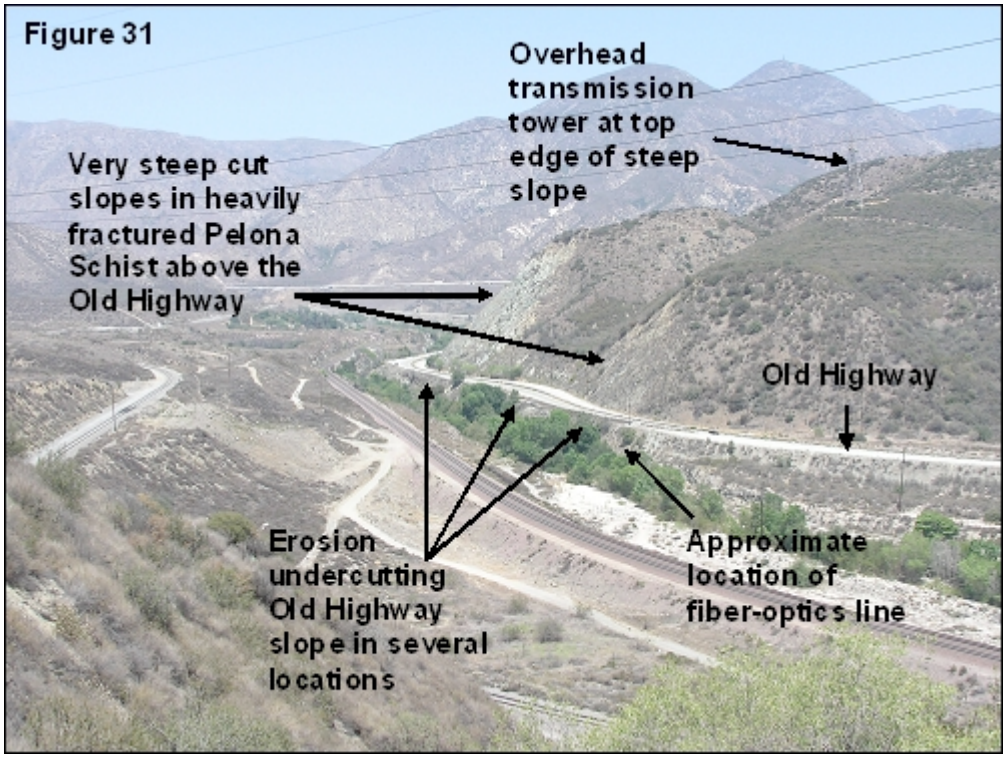

Scenario Earthquake Landslide Damage: As shown in Figure 32 below, a scenario would involve the failure and disruption of several lifelines. In addition to partial or complete failure of the slopes beneath and above the Old Highway, the other utilities that cross the area may also have significant damage (Figure 32). If the slope under the overhead powerline tower fails, the tower could also fail and be displaced over 50 meters downslope to the base of the hill. Likewise, if the slope below the Old Highway fails, the buried fiber-optics cable could be disrupted, failing into the adjacent drainage.

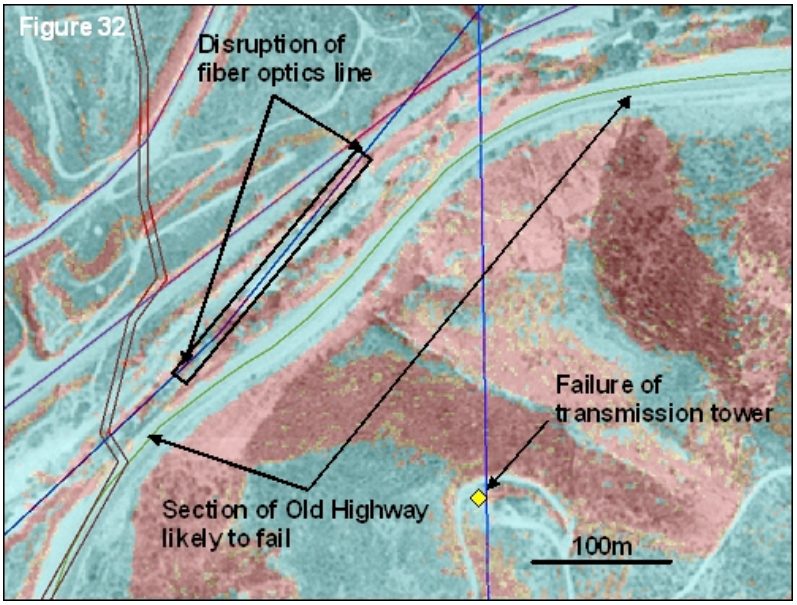

Area D: The steep, east-facing bedrock slopes along Cajon Canyon contain many landslides and weakened, east-dipping bedrock (Figure 33); a detailed analysis of landslide LS-1 in the central part of this slope was analyzed previously. If slopes in Area D fail, they could impact the railways, overhead transmission lines, and other buried utilities on or below the slopes. As shown in Figure 34, most of the east-dipping slope is identified as having a high landslide hazard potential. The specific lifelines that could be damaged by landslides include extensive portions of two railways.


Figure 33

Scenario Earthquake Landslide Damage: Under the worst possible scenario, there would be extensive failure of the slope in question, and damage to the lifelines in close proximity. The most severe damage would occur to the railways at the base of the slope, specifically the railway closest to the slope. An approximate three-kilometer length of this railway could be covered by up to 100,000 cubic-meters of slide debris, and possibly displaced several meters if undercut by the existing landslides along this slope. Because it is located further away from the slope, a smaller length of the second railway, approximately two-kilometers, could be covered by about 70,000 cubic-meters of slide material with less of a chance of being displaced by undercutting.

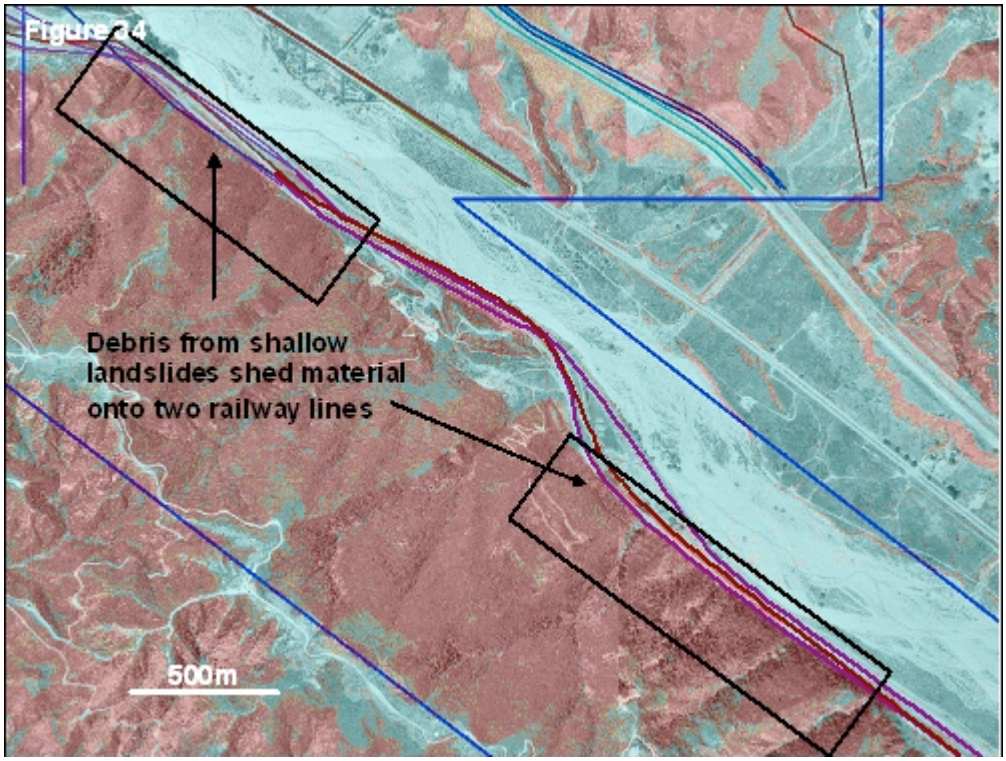

Area F: The steep slope areas adjacent to LS-2, located across the canyon from Blue Cut, are composed of eastward dipping Pelona Schist and ancient and/or questionable landslide deposits (Figure 35). Both Morton and Miller (2006) and Treiman (this study) mapped a landslide in the southern portion of Area F. However, in the northern portion, Morton and Miller (2006) map a large ancient landslide whereas Treiman questions whether a landslide exists in this area. In either case, the fact that this entire slope is fairly steep and underlain by weak Pelona Schist that adversely dips out of slope indicates that this area has a high hazard potential for landslides.

Scenario Earthquake Landslide Damage: There could be significant failure of the slope above the railway closest to the slope (Figure 36). The section of this railway that is to the north is about 400-meters in length and could have about 3,200 cubic-meters of slide debris deposited on it during the scenario earthquake. The railway section to the south is about 300-meters in length and could also have about 3,200 cubic-meters of slide debris deposited on it, and the possibility exists that this section of railway could be undercut by a landslide and displaced several meters to the east.

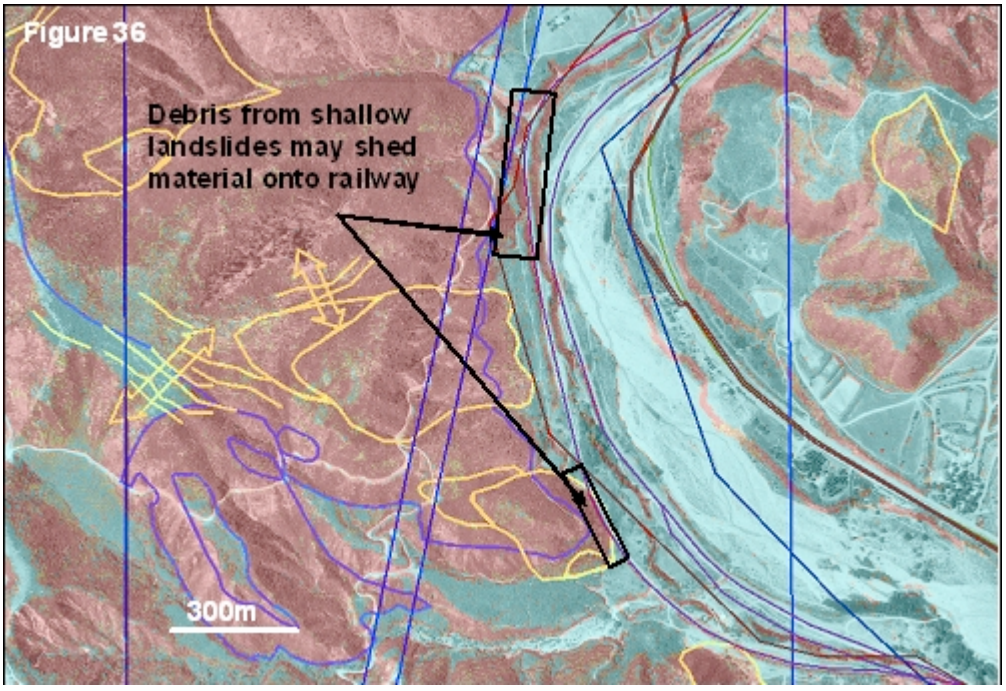

San Gorgonio Pass Focus Area

The San Gorgonio Pass focus area is located north of Palm Springs, along the eastern extent of the San Andreas Fault that ruptures in this scenario. Figure 37 shows the two specific areas that were analyzed for potential slope failure: 1) a tall (60-meter), steep slope, named LS-Bluff for this analysis, made up of late Pleistocene age Cabazon Fanglomerate, and 2) a large "landslump" mapped by Proctor (1968), known as LS-Slump, made up of Cabazon Fanglomerate also. A description of the geotechnical properties of the geologic materials that make up the two slopes evaluated is given in Table 8.

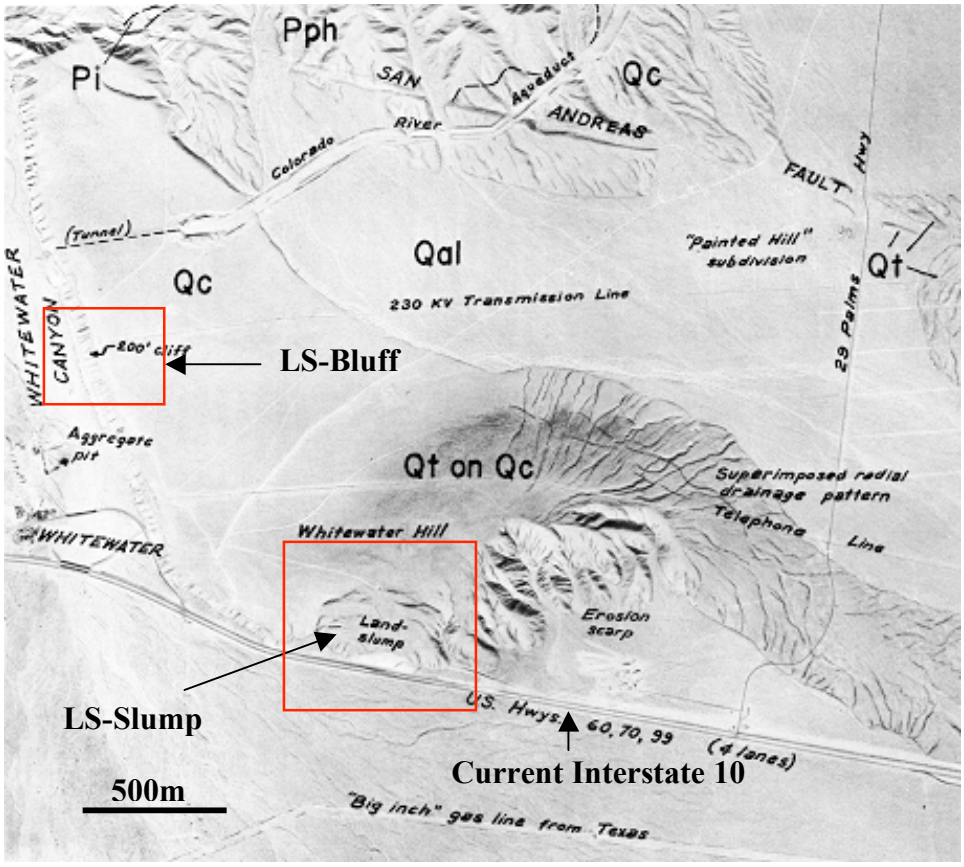

Figure 37. Vertical air photo of the Whitewater Canyon area at the eastern edge of the San Gorgonio Pass focus area, from Proctor (1968). The two areas evaluated for earthquake slope stability are indicated.

Table 8. Description of the geologic formations (Proctor, 1968) and their geotechnical attributes.

LS Name	Geologic Formation	Formation Description	General Rock Strength Characteristics
LS-Bluff	**Qc** = Cabezon Fanglomerate (late Pleistocene)	Ill-sorted, poorly bedded pebbly to bouldery tan arkosic sandstone/ conglomerate with lesser amounts of fresh-water limestone breccia.	The fanglomerate is moderately indurated, forming a 60-meter-high slope at about a 35° angle along the bluff in question. It has been our experience that similar material has a peak shear strength value of 38°, which is also close in value to the angle of repose of the slope.
LS-Slump	**Qc** = Cabezon Fanglomerate (late Pleistocene)	Ill-sorted, poorly bedded pebbly to bouldery tan arkosic sandstone/ conglomerate with lesser amounts of fresh-water limestone breccia.	The fanglomerate is moderately indurated, forming a 60-meter-high slope at about a 35° angle along the nearby bluff. However, material within the pre-existing land-slump is expected to be weaker because it has been disturbed/deformed. For this reason, the material within this land-slump was given a reduced shear strength value of 30°.

Evaluation of Slope at LS-Bluff

This slope stability analysis was performed to evaluate the stability of a steep, +60-meter-tall slope that has in close proximity (~30 meters) several overhead power-line towers. This slope has been down-cut by the Whitewater River over time. These towers and the slope are shown in the photos below (Figure 38).

(a) (b)

Figure 38. The 60-meter-high bluff showing (a) the close proximity of the overhead power-line towers to the edge of steep bluff slope, and (b) the steepness of the bluff slope. The material making up this slope is the late Pleistocene age Cabezon Fanglomerate.

Assumptions for Landslide Displacement Analysis: Several assumptions regarding the subsurface conditions were formulated for the analysis:

1. Though there is evidence nearby suggesting that this older alluvial slope is prone to landsliding, no failure planes were designated for this analysis.
2. The head of the modeled landslide was placed over 30 meters from the edge in the proximity of the overhead powerline towers to determine the potential for failure at that distance from the slope.
3. In our experience, older fanglomerate deposits similar to the Cabazon Fanglomerate, consisting of sand and gravel like this slope, has an angle of internal friction 38^{o} and a cohesion value of 0 kN/m^{3}. The values shown in Table 9 were used in our model.

Table 9. Material properties used in the stability and displacement analyses for site LS-Bluff.

Material	Angle of Internal Friction (degrees)	Cohesion (kN/m^{3}(pcf))
Cabazon Fanglomerate	38	0

LS-Bluff Analysis: Our analysis determined that a potential failure plane 30 meters from the edge is has a factor of safety of about 1.61. The landslide profiles for this analysis are shown in Appendix A as Figures A15 and A16.

Potential Landslide Displacement Calculations:

Input data:

Yield Acceleration = 0.22g
Average Thickness of Sliding Mass = 26m
Shear Wave Velocity of Sliding Mass = 390m/sec
Scenario Earthquake Magnitude (Mw) = 7.8
Site Peak Ground Acceleration (from PSHA) = 0.623g
Initial Fundamental Period of Sliding Mass = 0.27sec
Spectral Acceleration at Degraded Fundamental Period = 1.05g

Results:

Probability that Newmark Displacements are < 1cm = 0%
DISPLACEMENTS

Median Value	23cm
Minus 1 Sigma	12cm
Plus 1 Sigma	45cm

Scenario Earthquake Landslide Damage: Under the shaking conditions presented by the scenario earthquake, the median and maximum Newmark displacements of this failure were calculated to be about 0.3 and 0.5 meters, respectively. Based on these results, a catastrophic slope failure that includes these towers is unlikely. The worst-case potential for these towers is to be displaced about one-half meter towards the slope (west).

Evaluation of LS-Slump

This slope stability analysis was performed to evaluate the stability of a south-facing "landslump", known as LS-Slump in this analysis, formed in Cabazon Fanglomerate as mapped by Proctor (1968). Interstate 10 crosses directly below the base of LS-Slump and might be impacted by failure of this slope (Figure 39 and 40). Other utility lifelines that follow the I-10 corridor, two SCE utility lines and two Sprint fiber-optic lines, could also be impacted (Figure 40).

(a) (b)

Figure 39. Photos of LS-Slump showing (a) a partial profile of the landslide with I-10 in the foreground, and (b) the lateral extent of LS-Slump.

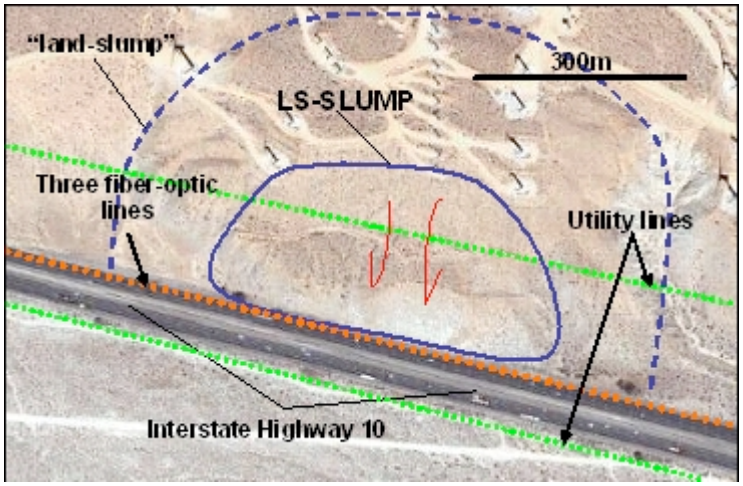

Figure 40: Satellite image showing the location of the "land-slump," mapped by Proctor (1968), and LS-Slump, just north of the I-10 highway. Location of several utility lifelines are also shown.

Assumptions for Landslide Displacement Analysis: Several assumptions regarding the subsurface conditions were formulated for the analysis:

1. The material that makes up the landslump has likely been deformed by landslide activity and, thus, has a reduced strength.
2. A slide plane consisting of weaker material was introduced at the head of the landslump. The dip of this material reflects the apparent dip of 25^{o} in the Cabazon Fanglomerate in this area.
3. In our model, the top of potential sliding bracketed the area where ground cracks can be seen in the air photo in Figure 41. This allows a larger area for the model to develop the top of the slide plane.
4. In our experience, older fanglomerate deposits similar to the Cabazon Fanglomerate, consisting of sand and gravel, has an angle of internal friction 38^{o} and a cohesion value of 0 kN/m^{3}. However, with the expectation that this material has been deformed, a value of 30^{o} was used in the analysis, as shown in Table 10.

Table 10. Material properties used in the stability and displacement analyses for site LS-Bluff.

Material	Angle of Internal Friction (degrees)	Cohesion (kN/m^{3}(pcf))
Cabazon Fanglomerate – deformed by landslide activity	30	0
Slide plane material	20	0

LS-Slump Analysis: Our analysis determined that the top of a potential failure plane would develop approximately 180 meters from the base of the slope, as shown in the landslide profiles in Appendix A as Figures A17 and A18. The static factor of safety for LS-Slump of about 1.53:

Potential Landslide Displacement Calculations:

Input data:

Yield Acceleration = 0.18g
Average Thickness of Sliding Mass = 30m
Shear Wave Velocity of Sliding Mass = 390m/sec
Scenario Earthquake Magnitude (Mw) = 7.8
Site Peak Ground Acceleration (from PSHA) = 0.623g
Initial Fundamental Period of Sliding Mass = 0.31sec
Spectral Acceleration at Degraded Fundamental Period = 0.99g

Results:

Probability that Newmark Displacements are < 1cm = 0%
DISPLACEMENTS

Median Value	31cm
Minus 1 Sigma	16cm
Plus 1 Sigma	60cm

Scenario Earthquake Landslide Damage: Under the shaking conditions presented by the scenario earthquake, the median and maximum Newmark displacements of this failure were calculated to be 0.3 and 0.6 meters, respectively. Based on these displacement values, it is unlikely that the entire landslide will fail catastrophically but that potential does exist. Because the nature of the ground cracks near the top of LS-Slump is not fully known, a conservative estimate for landsliding was considered. If the landslide was to have complete failure, the slide could bury I-10 and utility lines in approximately 1.5-million cubic-meters of debris, the total volume of the potential slide mass. There is also the potential that the slide plane of the landslide could undercut and displace I-10 and the utilities southward. Therefore, the most conservative scenario would involve complete failure of LS-Slump, not only displacing the highway and utilities to the south but also burying the area in 1.5-million cubic-meters of material. If catastrophic failure of LS-Slump doesn't occur, at least 45,000 cubic-meters of material could be shed from the steep slope, potentially covering the highway with debris and displacing one of the utility lines that exist within this slope.

Palmdale/Highway 14 Focus Area

The Palmdale/Highway 14 focus area is located about 8 kilometers south of the City of Palmdale. This focus area encompasses Highway 14, and several other lifelines for water, transportation, and petroleum products.

Within this focus area, the only significant slopes that could have impacts on lifelines are a pair of 20-meter-tall road cuts that face each other along Highway 14 within the two northern splays of the San Andreas Fault Zone. Landslide hazards caused by a large earthquake were evaluated previously by CGS for the Seismic Hazard Zone map of the area, specifically the zone map for the Ritter Ridge USGS 7.5-minute quadrangle (Figure 41; Wilson *et al*., 2003; DOC-CGS, 2003a and b); this method is described in the "shallow landslides" section for Cajon Pass. Based on that analysis, these road-cut slopes are considered to have a high hazard potential for landslides.

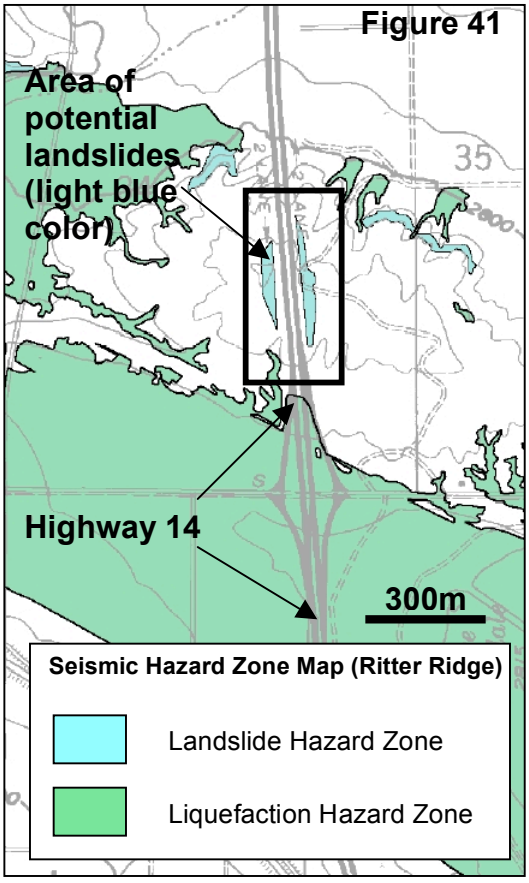

Scenario Earthquake Landslide Damage: The debris being shed from the slopes will be about one meter thick from the sides of the road cut. Based on this amount coming from the slopes, approximately 1,000 cubic-meters of material could be deposited on the highway during the scenario earthquake. Because of the narrow width of this portion of highway, all lanes would likely be covered by this landslide debris.

Interstate 5/Pyramid Lake Focus Area

The Interstate 5 highway corridor from Gorman to Pyramid Lake was examined for potential earthquake-induced landslide hazard. The priority targets identified for analysis are a large landslide complex and adjacent 60-meter-tall, slide-prone road cut near the Vista Del Lago Visitor Center (California Department of Water Resources facility) above Pyramid Lake, approximately 25 kilometers from the western end of the scenario fault rupture. This area has produced numerous recent landslides activated during winter rains that have impacted the highway and various utility lifelines that cross the area.

The peak ground motions estimated for the scenario earthquake are in the 0.16 to 0.21g range for the Pyramid Lake area [Ken Hudnut (USGS); ShakeOut version 1.1.0 dated July, 2007]. Based on a preliminary landslide analysis using these ground motions it was determined that ground shaking will be too low to trigger significant slope instability. Therefore, ground deformation from seismically induced landslides will not likely impact lifelines in this focus area.

Summary of Results and Limitations

Table 11 (below) summarizes the damage to lifelines.

AREA	LIFELINE	SUMMARY OF SCENARIO EARTHQUAKE LANDSLIDE DAMAGE
CAJON PASS		
LS-1	railway	displaced 10 meters to east; buried by 5.2-million cubic-meters of debris
LS-1	trans. towers	failure/collapse 50 meters to east
LS-1	petro. pipe	displaced 5 meters to east; buried by 5.2-million cubic-meters of debris
LS-2	railway	displaced 5 meters to east; buried by 4.7-million cubic-meters of debris
LS-2	trans. towers	failure/collapse 150 meters to east
LS-2	petro. pipe	displaced 10 meters to east; buried by 4.7-million cubic-meters of debris
LS-3	railway	displaced 0.3 meters to east
LS-3	railway	displaced 0.3 meters to east
LS-4	railway	buried by 2.5-million cubic-meters of debris
LS-4	trans. tower	failure/collapse 50 meters to north
LS-5	petro. pipe	displaced 0.3 meters to west
LS-5	unk. utility	displaced 0.3 meters to west
A	Interstate 15	failure/settlement of fill prism under highway up to several meters
B	trans. towers	failure/collapse 50 meters to north
B	petro. pipe	failure/displacement 10 meters to south
B	petro. pipe	failure/displacement 5 meters to south
C	Old Highway	displacement/failure/burial of highway downslope
C	trans. tower	failure/collapse 70 meters to north
C	fiber-optics	failure/displacement 10 meters to north
D	railway	displacement 3 meters to east; buried by 100,000 cubic-meters of debris
D	railway	buried by 70,000 cubic-meters of debris
E	Interstate 15	buried by 73,000 cubic-meters of debris
F	railway	displaced 3 meters to east; buried by 6,400 cubic-meters of debris
SAN GORGONIO PASS		
LS-Bluff	trans. towers	displacement 0.5 meters to west
LS-Slump	Interstate 10	displaced to south; buried by 1.5-million cubic-meters of debris
LS-Slump	unk. utility	displaced to south; buried by 1.5-million cubic-meters of debris
LS-Slump	fiber-optics	displaced to south; buried by 1.5-million cubic-meters of debris
INTERSTATE 14/ PALMDALE		
roadcuts	Interstate 14	buried by 1,000 cubic-meters of debris

- The earthquake record used to create the hazard potential map for the Cajon Pass focus area was the "Lucerne" record from the 1992 Landers Earthquake. Because this record is smaller in magnitude and PGA than that of the MHDP scenario earthquake, the calculated Newmark displacements, as well as the associated hazard-potential rankings displayed on the hazard potential map, are less conservative than if they were calculated from a record representing the scenario earthquake.

- As stated in this report, landslide debris volumes are upper-bound estimates that represent a "worst-case scenario." More realistic volume calculations would require significantly more information about the geologic conditions. There are a number of factors not analyzed by CGS due to time constraints:
    - Site-specific geotechnical information (soil moisture/ground water, rock strength, rock orientation/fractures/structures, etc.) would help identify the susceptibility for the failure of the existing landslides and steep slopes, and fine-tune the debris volume estimates.
    - The ability of any mitigative measures by lifeline operators to contain landslide debris is unknown.
    - The run-out distances of slide materials and, thus, the exact amount of debris that will impact lifelines are unknown.

- Saturated soil conditions caused by excessive rainfall would increase the likelihood of landslides in the focus area during a large earthquake. If the saturated soil conditions exist, the scenario for landslides could be worse than discussed in this report.

- Limitations of the Bray and Travasarou (2007) Method:
    - The Newmark displacement values provided in moderate- to deep-landslide section of this report are derived from the methodologies which consider the effects of the landslide mass on the ground motions traveling through it. For the relatively deep-seated landslides evaluated in this study this is the most appropriate methodology to use. However, the scenario earthquake magnitude, and presumably the associated near-field ground motions, exceeds that of the strong motion records used by Bray and Travasarou (2007) in developing their model. Therefore, the estimated displacements are extrapolations beyond the limits of the model. In addition, this evaluation relied heavily on estimated material parameters and subsurface geological conditions inferred from observed surficial geomorphology. With the high level of uncertainty in the conditions modeled in this study, and giving consideration to the additional limitations of the model and other factors described below, it generally may be appropriate to use displacement values near, or at the higher end of the estimated ranges.
    - The Bray and Travasarou (2007) simplified method attempts to account for the modifications to the vertically-propagating earthquake shaking in the landslide mass caused by landslide mass itself, and for the inertial forces caused by the landslide mass as it alternately sticks and slips during the seismic shaking. However, landslides which are long in length relative to the natural period of the

input ground motion do not "feel" the shaking as a uniform pulse. In such cases, different parts of the landslide may experience inertial forces in opposite directions at the same time so that the overall earthquake and gravity driving forces acting on the landslide slip surface do not exceed the overall resisting forces. Slope displacement estimates may be over-conservative where this phenomenon occurs.

- It has been observed in several recent earthquakes that existing deep-seated landslides often are not completely reactivated by earthquakes. Instead, most of the displacement occurs near the top of the landslide, the strains dissipate along its length and may not be apparent at the toe. The displacement manifests as numerous fissures and breaks in the ground surface, often defining the upper part of the landslide. In addition to the added stresses now applied to the lower portion of the slip surface, the fissures at the top of the slide can serve as conduits of surface water runoff into the landslide mass creating the potential for delayed failure, months to years after the earthquake.

- If ground displacements are large (greater than one meter) in an existing landslide there is the potential that the landslide could break up and change behavior from a sliding block to a flow-type failure. There are many factors that need to be considered to evaluate this potential (including density of discontinuities, water content, steepness and position on slope) that could not be evaluated in this study. However, one significant consequence of this change in failure mode is the distance that the landslide can travel after initiation. Rather than displacements of tens to hundreds of centimeters expected for a coherent sliding block, once a flow failure initiates displacements can be an order of magnitude greater, that is, on the order of tens to hundreds of meters.

References

Bray, J.D. and Travasarou, T., 2007, Simplified procedure for estimating earthquake-induced deviatoric slope displacements: Journal of Geotechnical and Geoenvironmental Engineering, ASCE, v. 133, pp. 381-392.

Department of Conservation - California Geological Survey (DOC-CGS), 2003a, Official Seismic Hazard Zone Map, Palmdale 7.5-Minute Quadrangle, Los Angeles County, California: CGS release date August 14, 2003; scale 1:24,000.

Department of Conservation - California Geological Survey (DOC-CGS), 2003b, Official Seismic Hazard Zone Map, Ritter Ridge 7.5-Minute Quadrangle, Los Angeles County, California: CGS release date August 14, 2003; scale 1:24,000.

FEMA, 1992a, Inventory of Lifelines in the Cajon Pass, California: Earthquake Hazard Reduction Series 60, 97 p.

FEMA, 1992b, Collocation Impacts on the Vulnerability of Lifelines During Earthquakes with Applications to the Cajon Pass, California: Earthquake Hazard Reduction Series 61, 110 p.

Fumal, T.E. and Tinsley, J.C., 1985, Mapping shear wave velocities of near-surface geologic materials: in, Evaluating Earthquake Hazards in the Los Angeles Region – An Earth Science Perspective, J.I. Ziony, ed., U.S. Geological Survey Professional Paper 1360, pp. 127-149.

Jibson, R.W., 1993, Predicting earthquake-induced landslide displacements using Newmark's sliding block analysis: Transportation Research Board, National Research Council, Transportation Research Record 1411, 17 p.

Jibson, R.W., Harp, E.L., and Michael, J.A., 1998, A method for producing digital probabilistic seismic landslide hazard maps: An example from the Los Angeles, California area, U.S. Geological Survey Open-File Report 98-113, 17 pp.

Jibson, R.W., Harp, E.L., and Michael, J.A., 2000, A method for producing digital probabilistic seismic landslide hazard maps, in Wasowski, J., Keefer, D.K., and Jibson, R.W. (eds.), Landslide Hazards In Seismically Active Regions: EGS XXIII General Assembly – Natural Hazards (NH) Group, April 20-24, 1998, Nice, France; special publication of *Engineering Geology*, December 2000, Volume 58, Nos. 3-4, pp 271-290.

McCrink, T.P. and Real, C.R., 1996, Evaluation of the Newmark method for mapping earthquake-induced landslide hazards in the Laurel 7-1/2 minute Quadrangle, Santa Cruz County, California: California Division of Mines and Geology Final Technical Report for U.S. Geological Survey Contract 143-93-G-2334, U.S. Geological Survey, Reston, Virginia, 31 p.

Morton, D.M., and Miller, F.K., 2006, Geologic map of the San Bernardino and Santa Ana 30' x 60' quadrangles, California: U.S. Geological Survey Open-File Report 2006-1217, 4 sheets (digital version).

Newmark, N.M., 1965, Effects of earthquakes on dams and embankments: Geotechnique, v. 15, no. 2, p. 139-160.

Proctor, R.J., 1968, Geology of the Desert Hot Springs-Upper Coachella Valley area, California: California Division of Mines and Geology Special Report 94, 50 p., 1 plate, map scale 1:62,500.

Rocscience Inc., 2007, SLIDE 5.0 landslide program.

Wills, C.J. and Clahan, K.B., 2006, Developing a map of geologically defined site-condition categories for California: Bulletin of the Seismological Society of America, v. 96, no. 4A, pp. 1483-1501.

Wilson, R.C. and Keefer, D.K., 1983, Dynamic analysis of a slope failure from the 1979 Coyote Lake, California, earthquake: Bulletin of the Seismological Society of America, v. 73, p. 863-877.

Wilson, R.I., Perez, F.G., and Barrows, A.G., 2003, Earthquake-induced landslide zones in the Ritter Ridge 7.5-Minute Quadrangle, Los Angeles County, California: *in* CGS Seismic Hazard Zone Report 083, pp. 21-41.

Youd, T.L., 1980, Ground failure displacement and earthquake damage to buildings: American Society of Civil Engineers Conference on Civil Engineering and Nuclear Power, 2d, Knoxville, Tennessee, 1980, v. 2, p. 7-6-2 to 7-6-26.

Appendix A: Slope Stability Analysis Figures Using the RocScience Inc. SLIDE Program (2007)

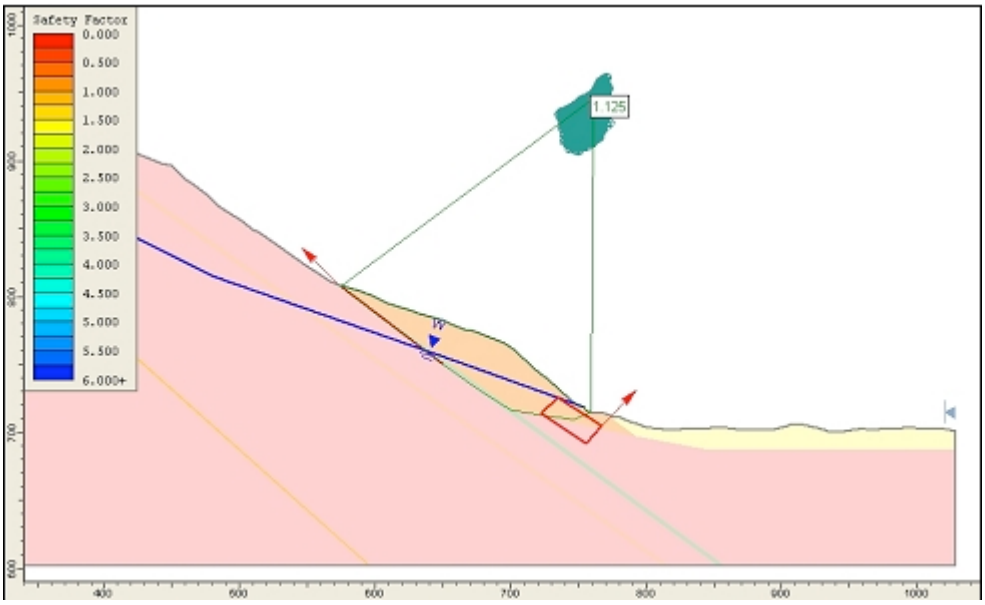

Figure A1. Cross-section for static slope stability analysis for Landslide LS-1A.

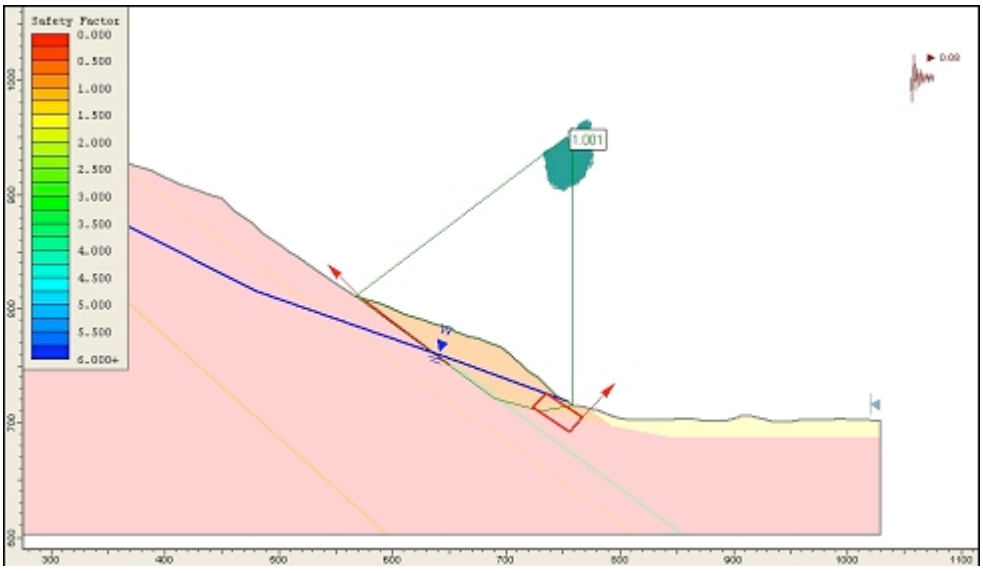

Figure A2. Pseudo-static analyses to determine the seismic coefficient for landslide LS-1A.

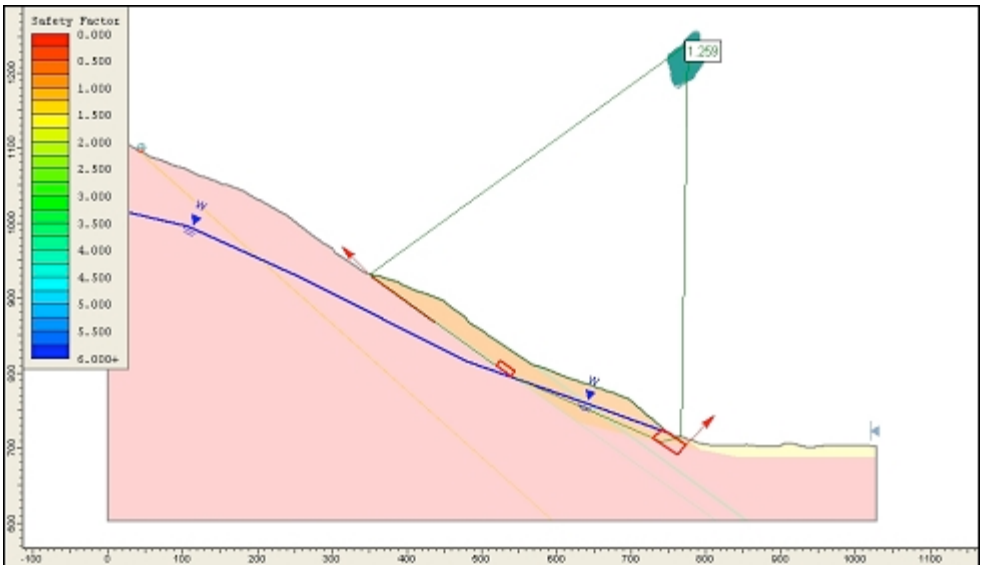

Figure A3. Static slope stability analysis result for Landslide LS-1B.

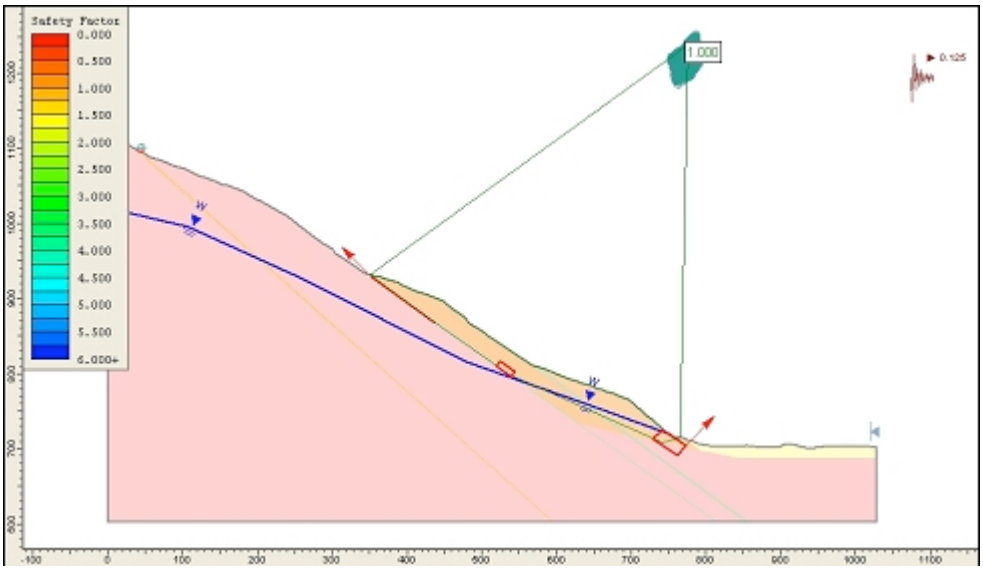

Figure A4. Seismic coefficient for Landslide LS-1B.

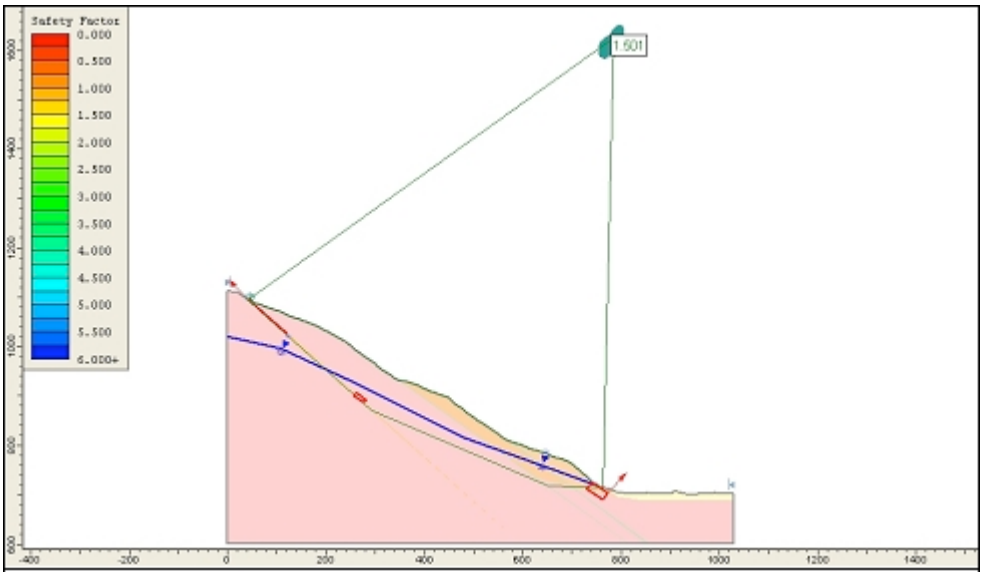

Figure A5. Static stability analysis results for Landslide LS-1C.

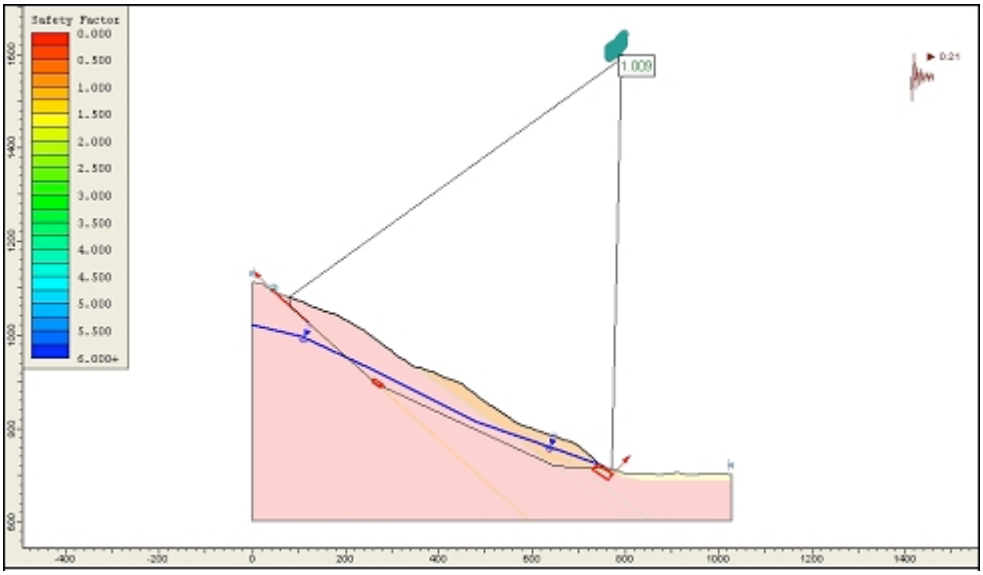

Figure A6. Seismic coefficient for Landslide LS-1C.

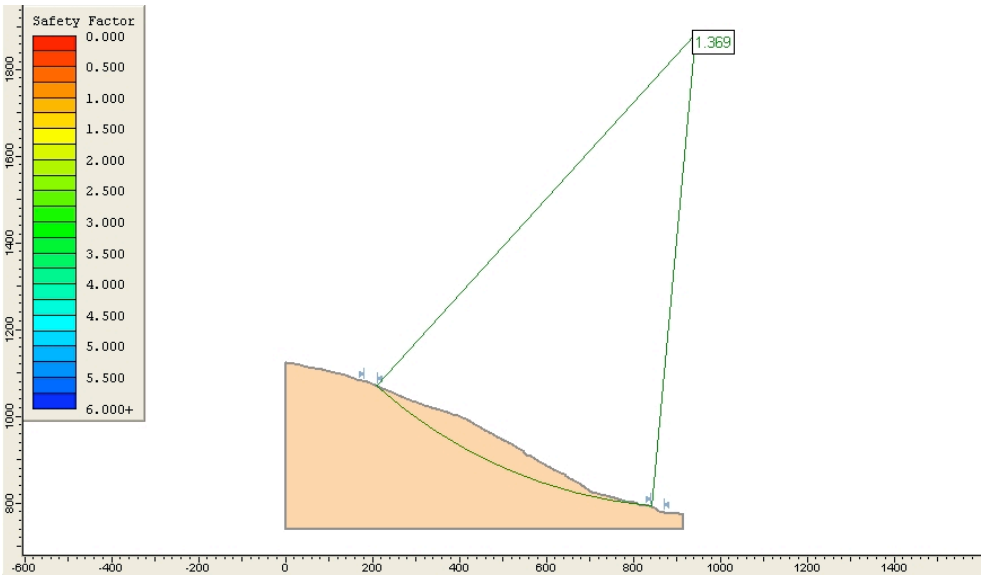

Figure A7. Static stability analysis results for Landslide LS-2.

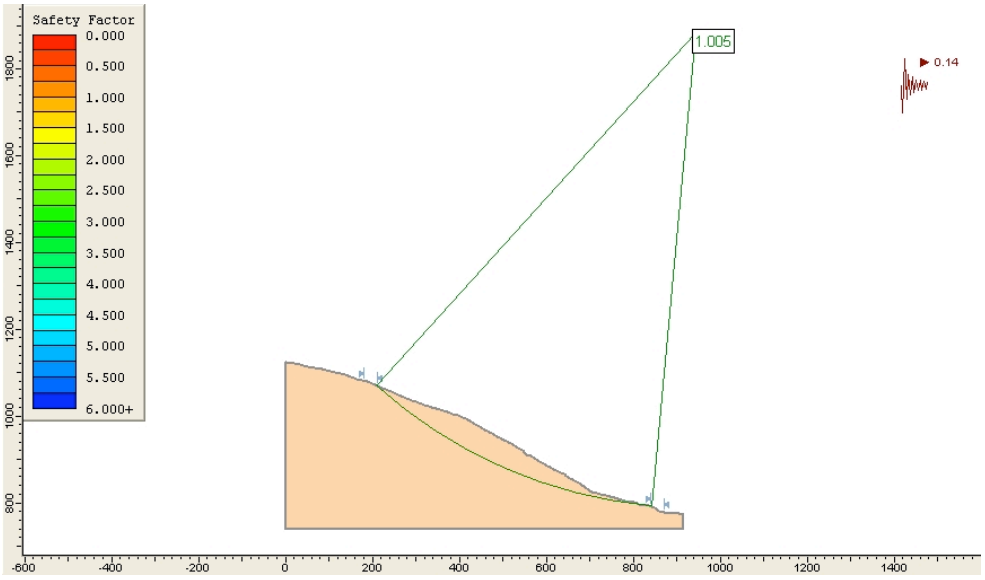

Figure A8. Seismic coefficient for Landslide LS-2.

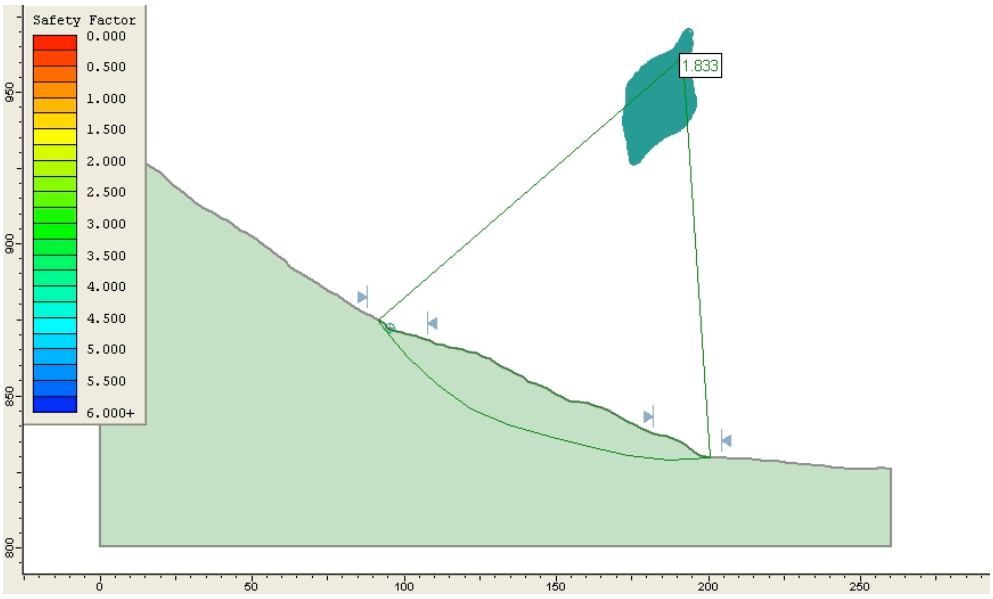

Figure A9. Static stability analysis results for Landslide LS-3.

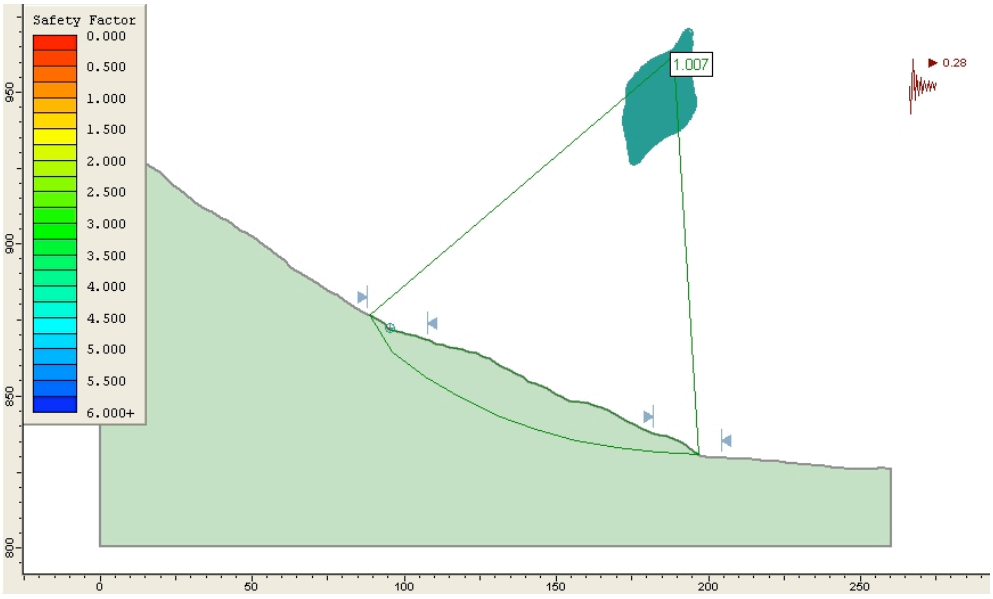

Figure A10. Seismic coefficient for Landslide LS-3.

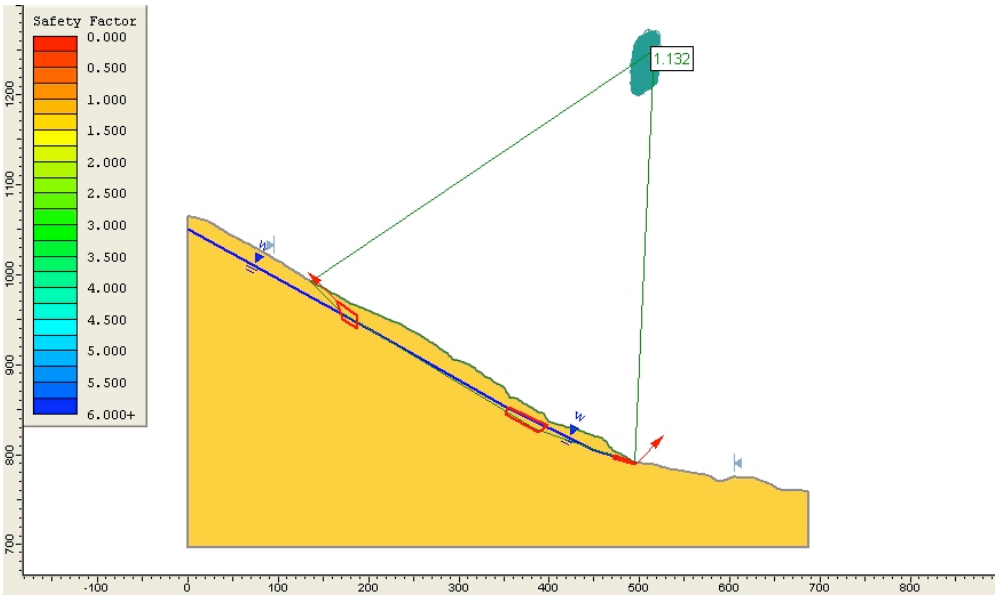

Figure A11. Static stability analysis results for Landslide LS-4.

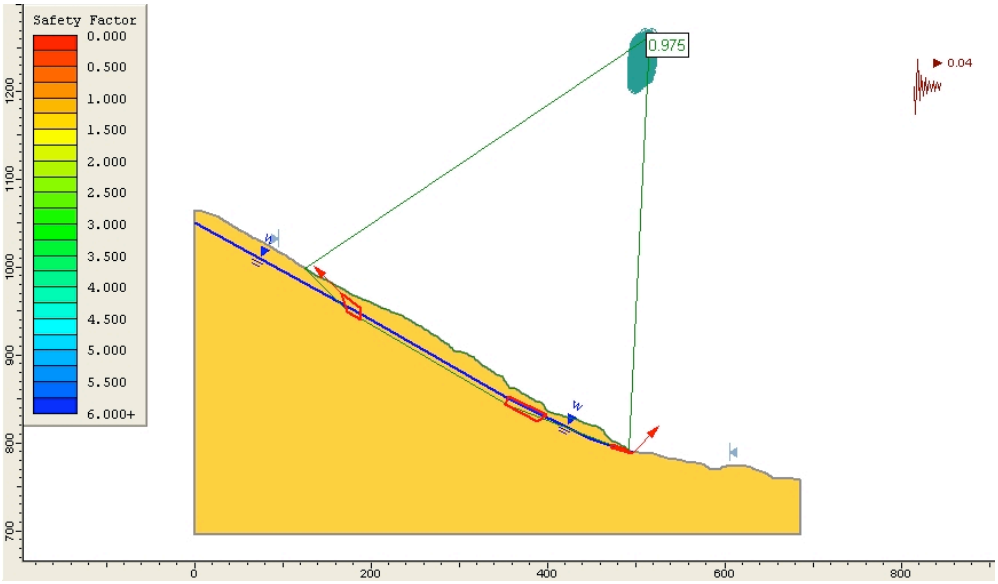

Figure A12. Seismic coefficient for Landslide LS-4.

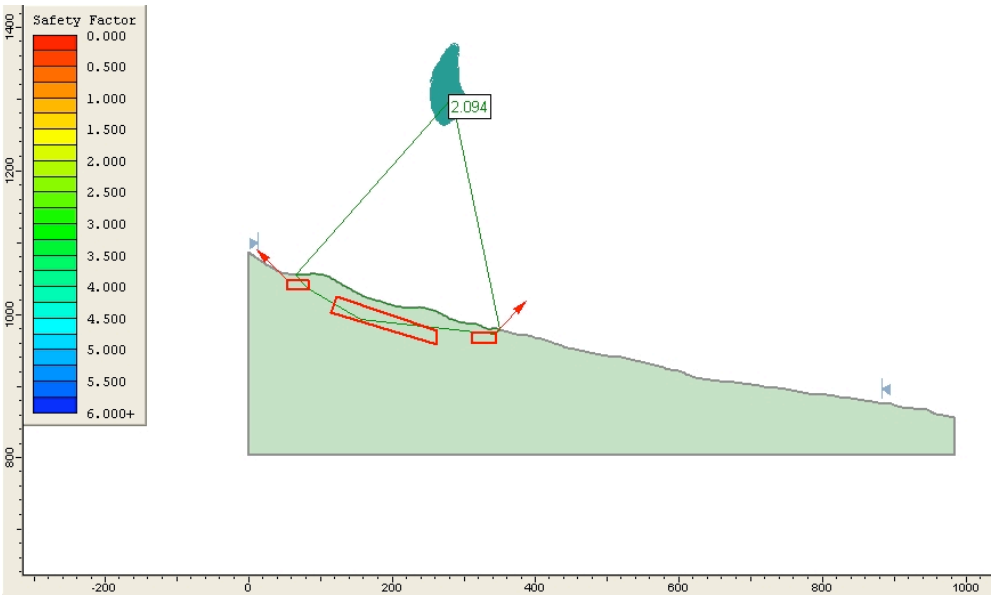

Figure A13. Static stability analysis results for Landslide LS-5.

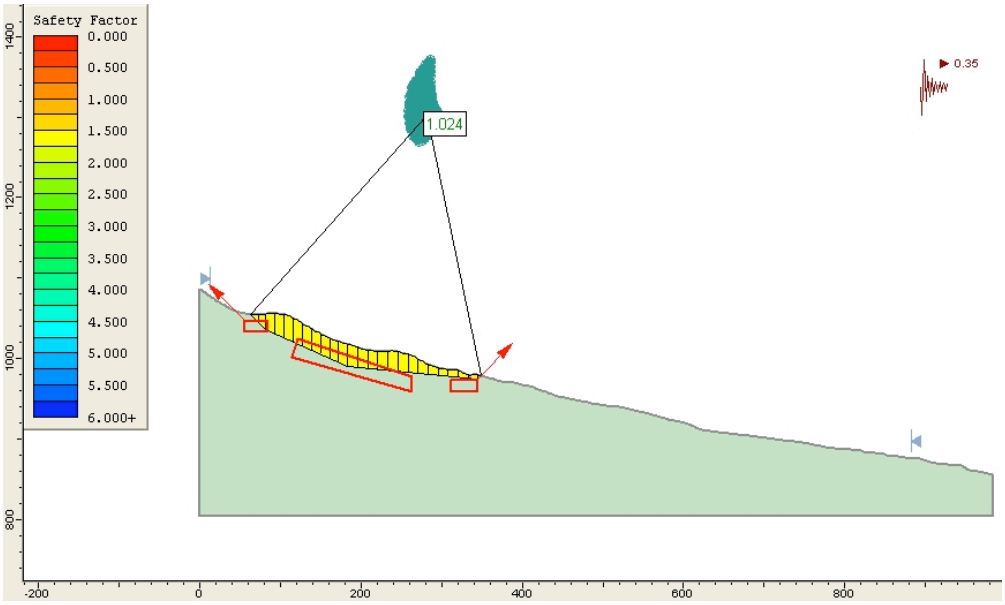

Figure A14. Seismic coefficient for Landslide LS-5.

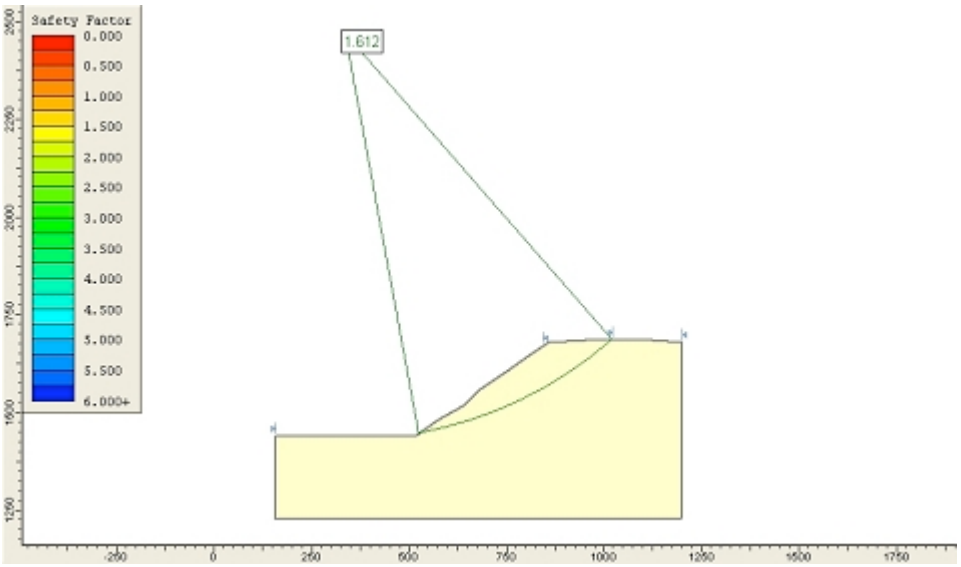

Figure A15. Static stability analysis results for site LS-Bluff in the San Gorgonio Pass focus area (distances shown are in feet).

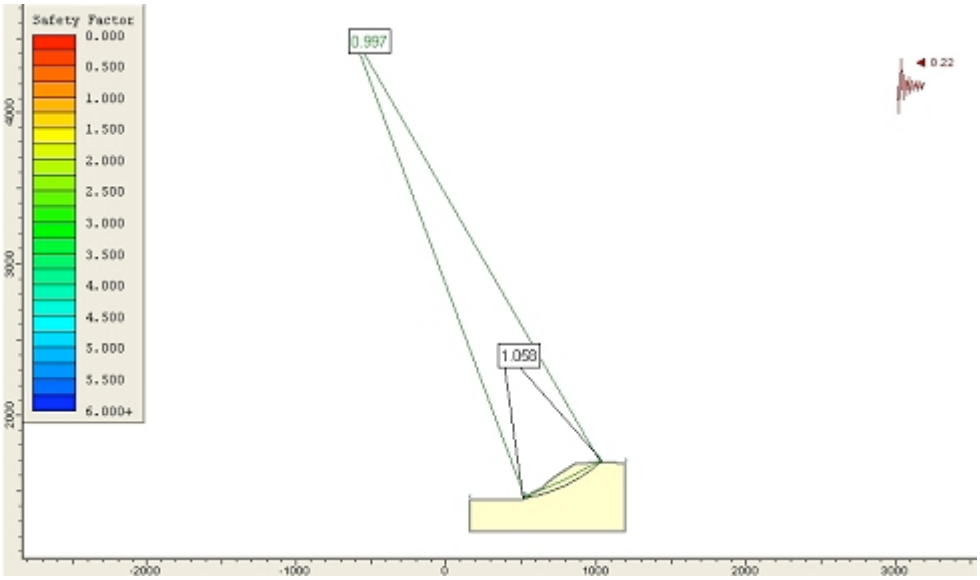

Figure A16. Seismic coefficient for site LS-Bluff in the San Gorgonio Pass focus area (distances shown are in feet).

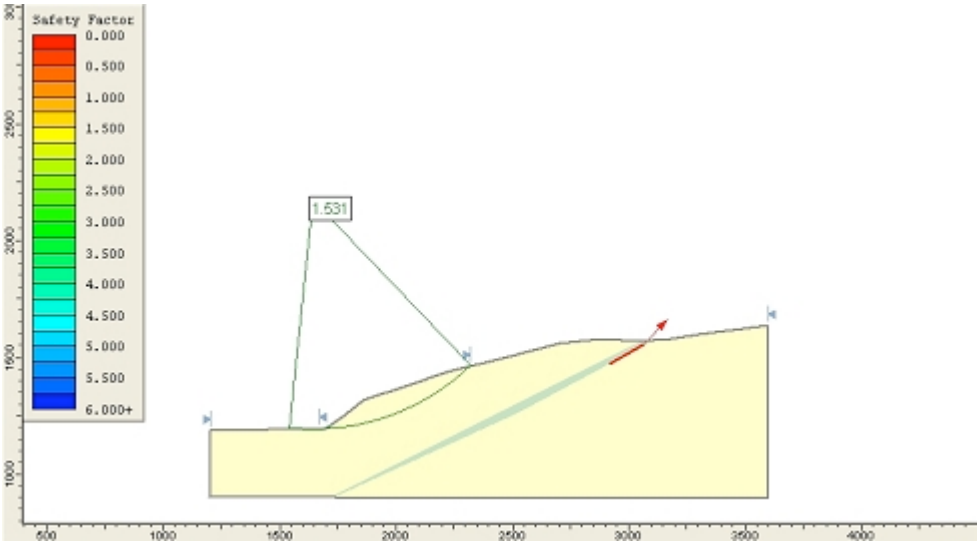

Figure A17. Static stability analysis results for site LS-Slump in the San Gorgonio Pass focus area (distances shown are in feet).

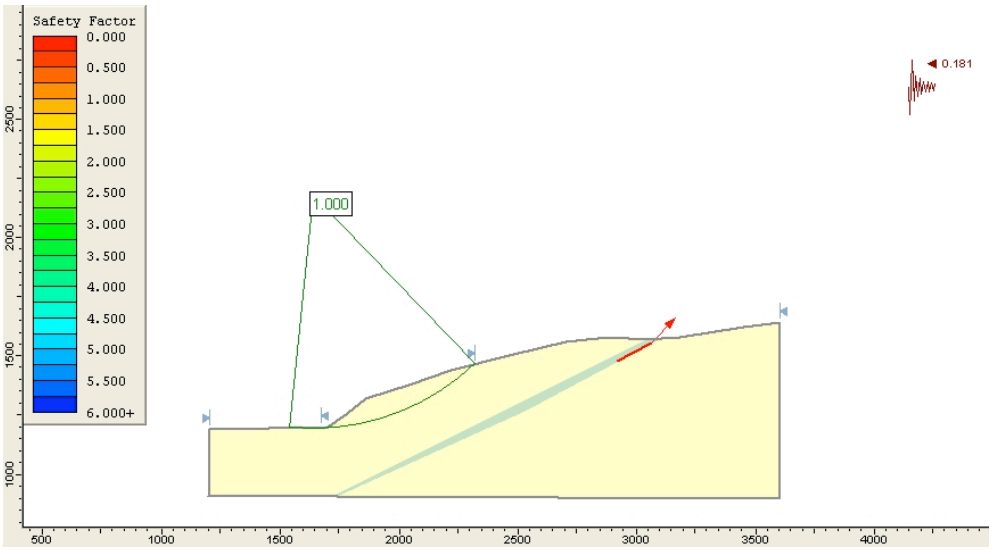

Figure A18. Seismic coefficient for site LS-Slump in the San Gorgonio Pass focus area (distances shown are in feet).